CHAPTER **6**

FIELD DATA ANALYSIS

6.1 INTRODUCTION

The current research is directed toward development of protocols and criteria for using a pavement's transverse surface profile to determine the layer contributing to surface distortion. Criteria have been proposed on the basis of theoretical predictions of pavement response and on the basis of analysis of available data identified in a literature search. The criteria include the net sum of positive and negative areas (determined within the bounds of a reference line), the surface profile, and the ratio of the positive and negative areas. The following sections present field data obtained by trenching pavements exhibiting rutting. These data are used to validate the proposed criteria or make adjustments to improve the criteria.

If, on a pavement transverse surface profile plot, a straight line is drawn between the end points, some portions will lie above the line and other portions will lie below. The area between the straight line and the profile portions lying above the line is defined as positive area. The area between the line and portions of the profile lying below the line is defined as negative area. These terms are illustrated in Figure 3-1. The total area, which is the absolute sum of positive and negative areas, and the ratio of positive to negative area are defined as distortion parameters. These distortion parameters are used to determine the layer contributing to pavement rutting. Rut depth referred to in this report is determined by the "wire" method and is the maximum distance from the surface profile to the "wire" (see Figure 3-2).

The Alabama, Minnesota, Mississippi, Nevada, North Carolina, Ohio, and Texas Departments of Transportation have provided data and assistance for this project. Data were also obtained from the trenching of in-service pavements and test sections on MnROAD. The Texas Department of Transportation trenched four SPS-1 sites in October 2000. The data were not available until the end of January 2001. The Indiana Department of Transportation proposed several sites, which were found by the research team to be unsuitable for the project.

A newly devised straightedge was used in measuring the trench profiles on the two sites in Mississippi and one site in North Carolina. A detailed description of this device is given in Section 6.9.

6.2 ALABAMA

Trenching data were obtained from 13 Alabama Department of Transportation (ALDOT) test sites [65]. The investigation focused on the causes of rutting in HMA pavements. After thoroughly reviewing data for the 13 sites, it was determined that three sites could be used for criteria validation in the current study: Sites 1 (no overlay), 2 (overlay), and 10 (overlay). Data from the other 10 sites could not be used primarily because the profiles did not span the full lane width, because transverse distance between elevation measurements was too great, or both. Some sites had been milled prior to profile measurement, rendering them unusable. The three usable sites were Site 1 on I-59 Southbound (mile post 27.3–32.4), Site 2 on I-59 Northbound (mile post 42.5–52.5), and Site 10 on US 78 Eastbound (mile post 61.9–66.5).

Trench profiles for usable sites are presented in Part A of Figures 6-1 through 6-3. These figures were scanned from Parker and Brown [65] because the data were not available in electronic format. The scanned figures were enlarged while the original aspect ratios were retained, and the data were then manually digitized. Failure modes were determined from the trench profiles. They were as follows:

- Site 1: HMA failure;
- Site 2: HMA failure; and
- Site 10: HMA failure.

When the data were in electronic format, the distortion parameters were determined using PAAP. The profiles and distortion parameters obtained through this process are presented in Part B of Figures 6-1 through 6-3. Failure modes determined by the criteria are also HMA failures (see Table 6-1). The ratio parameter values (i.e., the ratio of positive area to negative area) were high relative to those determined from the theoretical models. For example, the surface profile of Site 2 has a ratio of 10 (see Figure 6-2, Part B), while the typical value from theoretical analysis is less than 1. This difference suggests the existence of a lack of uniformity in construction (e.g., a hump at the lane center). This difference was also observed in data from other sites. Such a construction factor will not harm the use of the failure criteria because the criteria are conservative, as can be seen from the failure chart shown in Fig-

TABLE 6-1 Comparison of failure modes between criteria and field observation

Site	Rut Depth (mm)	Total Area (mm^2)	Ratio of Area	Failure by Criteria	Observed Failure	Agreement
Alabama, Site 1	12.5	249.5	1.04	HMA	HMA	Yes
Alabama, Site 2	12.2	14692.2	10.0	HMA	HMA	Yes
Alabama, Site 10	13.0	-4352.0	0.52	HMA	HMA	Yes
Mississippi, SH28E	26.1	12420.6	3.04	HMA*	Base	No*
Mississippi, SH302E	19.4	-21742.3	0.07	HMA	HMA	Yes
Minnesota, MnRoad Cell 4	10.0	5365.2	2.045	HMA	HMA	Yes
Minnesota, MnRoad Cell 16	5.9	406.5	1.161	HMA	HMA	Yes
Minnesota, MnRoad Cell 17	5.8	6050.3	7.217	HMA	HMA	Yes
Minnesota, MnRoad Cell 18	5.8	4261.9	3.639	HMA	HMA	Yes
Minnesota, MnRoad Cell 19	7.8	5016.8	3.077	HMA	HMA	Yes
Minnesota, MnRoad Cell 20	11.9	696.8	1.110	HMA	HMA	Yes
Minnesota, MnRoad Cell 22	6.7	11636.1	137.12	HMA	HMA	Yes
Minnesota, MnRoad Cell 23	14.3	-2380.6	0.746	HMA	HMA	Yes
Minnesota, MnRoad Cell 28	21.7	-1265.8	0.891	HMA*	Base	No*
Nevada, SR267	33.3	-41935.3	0.0	Base	Base	Yes
North Carolina, US64E	16.7	5257.8	2.005	HMA	HMA	Yes
Ohio, Site 390101, Station 1-50	13.5	-20657.8	0.0	Base	Base	Yes
Ohio, Site 390101, Station 4-00	15.4	-16457.1	0.0	Base	Base	Yes
Texas, IH10WB Site 3	39.6	-64335.3	0.013	Base		N/A
Texas, IH20WB Site 1	24.2	-13935.4	0.181	HMA		N/A
Texas, SH34 Site 1	21.8	-46451.5	0.0	Subgrade		N/A
Texas, US77-83 Site 2	23.0	-37857.9	0.0	Base		N/A
Texas, US281, Section 480161	19.2	9448.8	2.98	HMA	HMA	Yes
Texas, US281, Section 480162	23.1	13309.6	2.75	HMA	HMA	Yes

* The failure determined by the criteria is not the same as field observation. This discrepancy happens to pavement structures with a thin HMA layer (less than 75 mm [3 in.]). This discrepancy is treated as a special case and will not be dealt with by comparing the distortion parameters.

ure 6-4, where all HMA failure points except one are above the average trend line.

6.3 MISSISSIPPI

The Mississippi Department of Transportation (MDOT) identified two rutted pavement sections. One, SH 302, carries by-pass truck traffic from US 72 to I-55 south of Memphis, about 7 mi. This pavement exhibited significant rutting. A second section, SH 28, is located just east of Fayette, Mississippi. Logging trucks are a major component of the truck traffic. Rutting at some locations was severe. The trench site was located to avoid the more severely distorted areas.

6.3.1 SH 302 East

The trench was excavated July 10, 2000, and is located on SH 302 Eastbound, between Southhaven and Olive Branch, Mississippi (see Figure 6-5). The road is a four-lane pavement with an additional turning lane at the trenching site. The trench was excavated in the truck (i.e., outside) lane. Advantage was taken of the pavement width at this site to better observe the transverse extent of pavement distortion. Consequently, the trench was extended 250 mm (10 in.) beyond the centerline and 550 mm (22 in.) into the shoulder.

The pavement at the site consists of 80 mm (3.2 in.) of HMA layer, 230 mm (9 in.) of asphalt-treated base, 330 mm (13 in.) of subbase layer, and a subgrade layer. At this site, the straightedge was set at the trench edge and spanned the lane. A tape was used to measure from the top of the straightedge to the pavement surface and interface between each layer. Measurements were made at 25-mm (1-in.) intervals in the transverse direction. Profiles for the surface and layer interfaces are plotted in Figure 6-6, Part A. Close examination of the enlarged trench profile showed that rutting occurred predominantly in the HMA layer, with a minor contribution from the base layer. On-site visual inspection using a string line indicated that no pavement failure was present below the base layer.

The distortion parameters for the pavement surface are shown in Table 6-1 and Figure 6-6, Part B. The ratio of area is 0.07, indicating an HMA failure. This result agrees with the field observations. The small area ratio value is close to the dividing line between HMA and base failure. In fact, there was a small amount of rutting observed in the base.

6.3.2 SH 28 East

A trench was excavated in this pavement section on July 12, 2000. The site is 1.6 km (1.1 mi.) east of the SH 33 junction (see Figure 6-7). The road is a two-lane pavement with gravel shoulders. Severe rutting was found at the site. As noted pre-

viously, the trench location was selected to avoid more severe distortion.

In locating a suitable trench site, a string line was first stretched across the pavement surface. The surface rutting was clearly seen by the string shadow (see Figure 6-7, Parts B and C). The surface profile suggests failure in the HMA layer in terms of curvature reversal, which is a general characteristic of HMA rutting. However, the trench profiles show that rutting occurred in the base layer. This site, therefore, became a special case.

The pavement consists of 30 mm (1.2 in.) of HMA layer, 180 mm (7 in.) of asphalt-treated base layer, 180 mm (7 in.) of subbase layer, and a subgrade layer. At this site, the straightedge was set up to span from the pavement centerline to past the outside edge of the pavement. Measurements were made from the top of the straightedge to the pavement surface and layer interfaces. The data are shown in Figure 6-8, Part A. Close examination of the enlarged trench profile showed that rutting occurred primarily in the base layer. This occurrence was verified by on-site visual inspection using a string line; no rutting was found below the base layer.

Distortion parameters for the pavement surface profile were calculated and are shown in Table 6-1 and Figure 6-8, Part B. The ratio of area is 3.0, which indicates an HMA failure. However, the field observations and trench profile indicated a base failure. The thin HMA surface layer (less than 38 mm [1.5 in.] thick) may be the cause of the discrepancy. Previous finite element analysis on a low-volume structure having a 50-mm (2-in.) HMA surface layer gave similar results. The findings from this site are important in that they confirm the results of finite element analysis. Given the results, it appears that pavement structures with less than a 75-mm (3-in.) HMA layer must be dealt with as a special case.

6.4 MINNESOTA (MnROAD)

The Minnesota Department of Transportation (MnDOT) provided trench profiles for nine MnROAD test cells [66]. These transverse profiles were measured continuously with a rolling profilograph. Figure 6-9 shows the trench for Cell 28.

An analysis was performed on the MnROAD trench data for Test Cells 4, 16–20, 22, 23, and 28. The transverse surface profiles associated with these cells were obtained from data in an Excel file and are shown in Part A of Figures 6-10 through 6-18, respectively. Part B of Figures 6-10 through 6-17 shows the corresponding profiles at each pavement layer interface for the same cells (except Cell 28, which does not have layer interface data).

The surface profiles in Part A of Figures 6-10 through 6-17 appear to incorporate features that could affect calculated profile distortion parameters. Several of the profiles show considerable humps between the wheel paths. This phenomenon could simply be due to upheaval between the wheel paths with shear failure in the pavement. However, the humps could also be the result of a crown built into the surface. Part A of Figures 6-14 and 6-15 shows an example of such a hump. MnDOT personnel verbally confirmed the existence of crowns at the center of the 3.7-m (12-ft) lanes.

Accuracy of calculated distortion parameters is highly sensitive to the profile end-point elevations. In the initial analysis, the profile end points for the inside edge of the driving lanes were extrapolated for Cells 16–19 because the end points were not in the original MnDOT data set. As a result, there appeared to be a sudden jump in the profiles.

Personnel at MnDOT were contacted about the availability of more complete data sets. However, none of the profiles started from the centerline. After further study, it was decided that it would be inappropriate to extrapolate the data points to the pavement centerline. Thus, all the distortion parameters were calculated using profiles a few centimeters narrower than the 3.7-m (12-ft) lane. The distortion parameters for Cells 4, 16–20, 22, 23, and 28 were input into the criteria table, and the results are shown in Table 6-1 and Figure 6-4. With the exception of Cell 28, both the failure criteria and field observations indicate that rutting occurred in the HMA layer. The crowns in the pavement lanes cause all the surface profile distortion parameters to plot above the HMA failure trend line. This position above the HMA failure trend line means that the failure criteria are conservative.

The failure criteria indicated that Cell 28 has an HMA failure. This indication contradicts the field observation (i.e., that the failure was in the base). The HMA layer for this pavement is only 69 mm (2.7 in.) thick. As a result, deformations occur in the underlying layer. This case is similar to that of SH 28E in Mississippi. Again, this result further supports the validity of the finite element analysis method developed in this research.

6.5 NEVADA

The Nevada Department of Transportation (NDOT) excavated a trench on State Route 267 (SR 267) in southern Nevada. Figure 6-19 shows photographs of the trench and profile measurement process. This two-lane pavement structure consisted of 76 mm (3 in.) of HMA resting on 500 mm (20 in.) of base and 300 mm (12 in.) of subbase, as shown in Figure 6-20, Part A. Transverse profile measurements were taken at an increment of 25 mm (1 in.) over a pavement width of 3.3 m (130 in.) and were provided in electronic format. The data were entered into PAAP. Analysis results are shown in Figure 6-20, Part B. Both the calculated surface profile distortion parameters and field observations identified a base course failure. Thus, the predicted and observed failure modes were in agreement.

6.6 NORTH CAROLINA

The North Carolina Department of Transportation (NCDOT) excavated a trench in the westbound lane of US 64 East near Ashboro, North Carolina. Trenching operations are

shown in Figure 6-21. The pavement is a four-lane road with HMA shoulders. Falling Weight Deflectomenter (FWD) and coring data were collected prior to trenching.

The original pavement surface had been milled and replaced after rutting first occurred. The original pavement consisted of 125 mm (5 in.) of HMA layer (50 mm [2 in.] surface + 75 mm [3 in.] binder), 250 mm [10 in.] of base layer, and a subgrade layer. Data were collected from the pavement centerline to the lane edge on top of the overlay, the overlay/binder interface, the binder/base interface, and the base/subgrade interface. The resulting profiles are shown in Figure 6-22, Part A. Because the interface between the old surface and the binder is not clear (i.e., cannot be distinguished only by aggregate size), the data for this interface are not considered reliable. A visual inspection using a string line indicated no rutting below the binder course. Visual observation also indicated that rutting occurred in the surface and binder layers.

The calculated surface profile distortion parameters are shown in Figure 6-22, Part B. Both the calculated surface profile distortion parameters and field observations identified an HMA surface course failure. Thus, the predicted and observed failure modes were again in agreement.

6.7 OHIO

The Ohio Department of Transportation (ODOT) provided data from an LTPP SPS-1 section [67]. The section number for this site is 390101. The site consists of 175 mm (7 in.) of HMA and 200 mm (8 in.) of dense-graded aggregate base on the subgrade. Three trenches were excavated at Stations 1 + 50, 2 + 65, and 4 + 00. Extensive cracking existed at Station 2 + 65. As a result, data from this trench were not included in the analysis. Part A of Figures 6-23 and 6-24 shows the surface profiles observed immediately after construction and as a function of time at Stations 1 + 50 and 4 + 00, respectively. The profile data were input into PAAP, and the results are presented in Part B of Figures 6-23 and 6-24. Base failure was predicted by the distortion parameters. ODOT confirmed that failure occurred in the base. Thus, the predicted and observed failure modes were in agreement.

ODOT also provided data for two LTPP SPS-8 sections: 390803 and 390804. The two pavements had cross sections of 100 mm (4 in.) of HMA and 200 mm (8 in.) of dense-graded aggregate base, and 175 mm (7 in.) of HMA, and 300 mm (12 in.) of dense-graded aggregate base, respectively. The subgrades of both pavements were similar.

The data were provided in paper format and were manually digitized. Trench profiles for Section 390803 are shown in Figure 6-25. Data for Section 390804 were not usable because of the poor quality of the original trench profiles. Field observations assigned the failure in Section 390803 to the base course. However, a decision was made to not use the section in criteria validation because the measured profile width was 3.0 m (10 ft) rather than 3.7 m (12 ft). Figure 6-25, Part A, has two missing points on the surface profile: one at the inner lane edge and the other at the outer lane edge. These missing data are likely to have higher elevations than the existing edge points. Therefore, the calculated distortion parameters will not accurately reflect the failure mode.

6.8 TEXAS

The Texas Department of Transportation (TxDOT) provided data taken from several trenched pavements [68]. Surface profile data were provided in an electronic format. The surface profiles were measured using a rod and level, as well as a Face Dipstick.® The rod and level data were used for analysis because the elevations were obtained at 150-mm (6-in.) increments while Dipstick data were obtained at 300-mm (12-in.) increments.

The electronic profile data were analyzed with PAAP. Resulting profiles and distortion parameters are presented in Figures 6-26 through 6-29. The failure modes predicted for each site based on the distortion parameter criteria were as follows:

- IH 10 WB, Site 3: base failure;
- IH 20 WB, Site 1: HMA failure;
- SH 34, Site 1: subgrade failure; and
- US 77-83, Site 2: base failure.

Unfortunately, the data supplied were not detailed enough be beneficial. Additional information was requested from TxDOT, but this information was also not beneficial. It was, therefore, not possible to use these data in the criteria validation.

In October 2000, TxDOT performed trenching operations on four SPS-1 test sections on US 281, Hidalgo County, Texas [69]. These test sections were built in 1997 and were part of 20 sections. The four trenched test sections were 480113, 480122, 480161, and 480162. Because there was no rutting observed for Sections 480113 and 480122, only the data for Sections 480161 and 480162 were used.

Fieldwork on Section 480161 began on 4 October 2000 (see Figure 6-30). The trench was located in the southbound driving lane of US 281. It was a four-lane divided pavement with 3.7-m (12-ft) wide lanes. The cross section at this location consisted of a 125-mm (5-in.) HMA layer (placed in two lifts), a 220-mm (8.5-in.) base layer (lime rock asphalt [LRA]), and a stabilized subbase layer.

Figure 6-31, Part A, shows the trench profiles at the HMA surface, the bottom of the top HMA lift, the bottom of the second HMA lift, the LRA bottom, and the bottom of the stabilized layer. Figure 6-31, Part B, gives the magnified surface profile; the corresponding distortion parameters are as follows:

- Maximum rut depth: 19.2 mm (0.76 in.);
- Total area: 9,448.8 mm^2 (14.6 $in.^2$); and
- Ratio of area: 2.98.

Using the failure criteria developed by the research team, it was determined that this section rutted because of an HMA failure. The data point corresponding to this section is shown on the failure chart in Figure 6-4. The 480161 data point is the leftmost circled point on the chart; the right one is for Section 480162. Actual failure for Section 480161 was determined to be an HMA failure; TxDOT personnel confirmed this using field observations.

Section 480162 is immediately north and adjacent to Section 480161. Trenching on Section 480162 also began on 4 October 2000 (see Figure 6-32). The pavement at this section consisted of a 125-mm (5-in.) HMA layer (placed in two lifts), a 220-mm (8.5-in.) base layer (crushed stone aggregate base [CSAB]), and a stabilized subbase layer.

Figure 6-33, Part A, shows the trench profiles at the HMA surface, the bottom of the top HMA lift, the bottom of the second HMA lift, the CSAB bottom, and the bottom of the stabilized layer. Figure 6-33, Part B, gives the magnified surface profile; the corresponding distortion parameters are as follows:

- Maximum rut depth: 23.1 mm (0.9 in.);
- Total area: 13,309.6 mm^2 (20.6 $in.^2$); and
- Ratio of area: 2.75.

According to the failure criteria, this section rutted because of an HMA failure. The data point for this section is also shown in Figure 6-4. TxDOT personnel confirmed that failure occurred in the HMA layer using field observations.

6.9 STRAIGHTEDGE DEVICE

In order to measure transverse profiles in an efficient and accurate way, the research team devised a straightedge device. The device was designed to be lightweight, easy to assemble, and very stable and to facilitate fast measurement of pavement surface and layer interface profiles. These features were helpful in meeting the requirement that trenching operations must be conducted in a single working day. Figures 6-34 through 6-38 show an overview and some details of the straightedge. A trench cross section and a plan view of a trench showing how the device was set up are shown in Figures 6-39 and 6-40, respectively.

The straightedge is 4.9 m (16 ft) long and consists of four 1.2-m (4-ft) sections. It is made of 50 × 50 mm (2 × 2 in.) aluminum box beam with a wall thickness of 3 mm (⅛ in.). The joint connections (tight sleeve connections with anchor) are rigid such that a perfect straightedge exists when the joints are secured with large thumbscrews. Adjustable legs are used on each end of the straightedge, along with 150 × 250 mm (6 × 10 in.) base plates. An additional adjustable leg is incorporated at the midpoint of the straightedge to serve two purposes: to ensure that the reference is level and to serve as a safety feature in case someone inadvertently applies excess pressure to the straightedge.

An aluminum alloy was used because it is both rigid and lightweight. Thermal expansion was checked using an expansion coefficient of 23.5×10^{-6}/°C and a maximum temperature change of 33.3°C (60°F). The total change in length under these extreme conditions would be 3.8 mm (0.15 in.). This small change in length guarantees that accuracy in the transverse direction will not be significantly affected by temperature changes that might occur in a single day.

6.10 SUMMARY

Table 6-1 includes the data and distortion parameters for the various field sites included in the study. The layer failures predicted by the modified criteria are in good agreement with the observed field results. However, there were two exceptions: Mississippi SH 28E and MnROAD Cell 28. In these cases, the HMA surface is inadequate to protect the base, causing the base to fail. Because of the base layer proximity to the surface, the surface distortion makes the failure appear to be in the HMA layer. These two pavements are similar in that the HMA layer is less than 76 mm (3 in.). This type of failure was predicted by the FEM analysis, and, consequently, the field results are valuable because they validate the theoretical analysis component of the study.

In the analysis, PAAP is used to determine rut depth, distorted areas, and ratio of area. Input for PAAP is the transverse surface profile for the pavement section. Subsequently, a spreadsheet that was developed as part of the analysis assigns the failure mode on the basis of the criteria represented in Figure 6-4 (see Chapter 5 for details). Figure 6-4 is a combined plot of FEM-predicted results and field data from Table 6-1. Trend lines for the layer failure modes are also shown in the plot.

It should be noted that the proposed criteria are conservative for the HMA failure mode. This trait can be seen in Figure 6-4, where all but one of the points corresponding to HMA failure are above the average line for HMA failure, as determined from the FEM analysis. The reason for this above-average position is that real pavements may include some feature variations not included in the ideal pavements of the theoretical analysis (e.g., a crown in the middle of a lane).

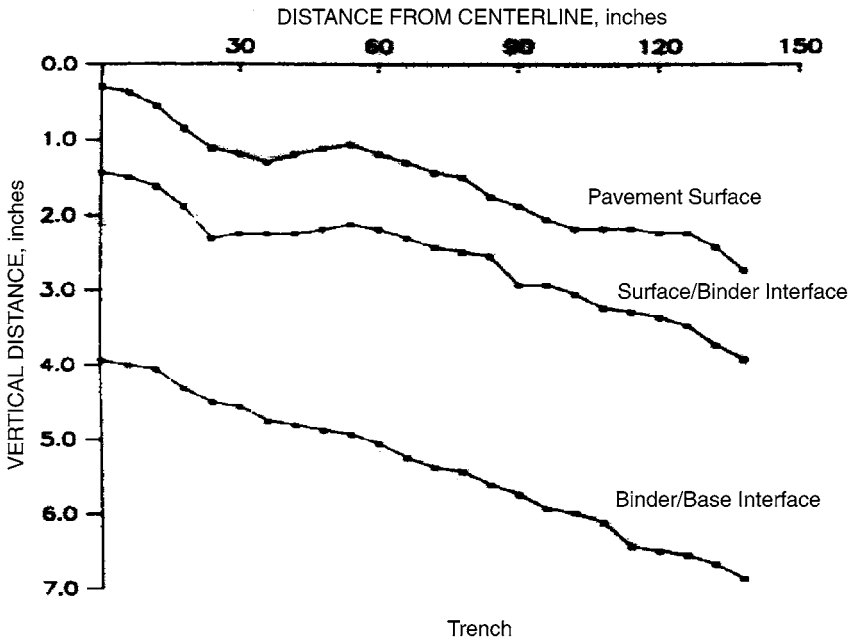

(a) trench profiles

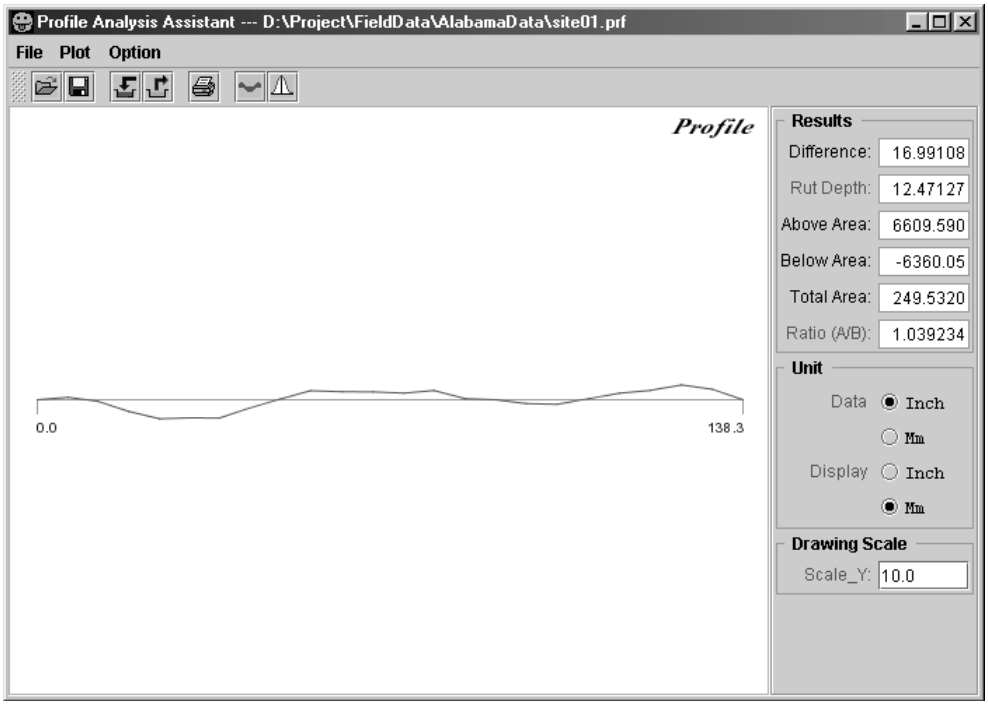

(b) surface profile and distortion parameters

Figure 6-1. Profiles of Alabama Site 1.

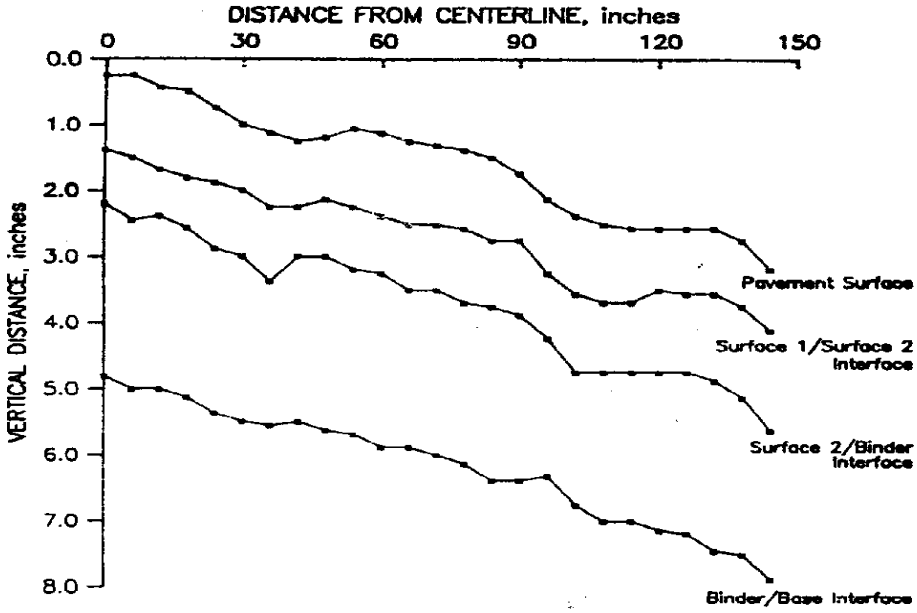

(a) trench profiles

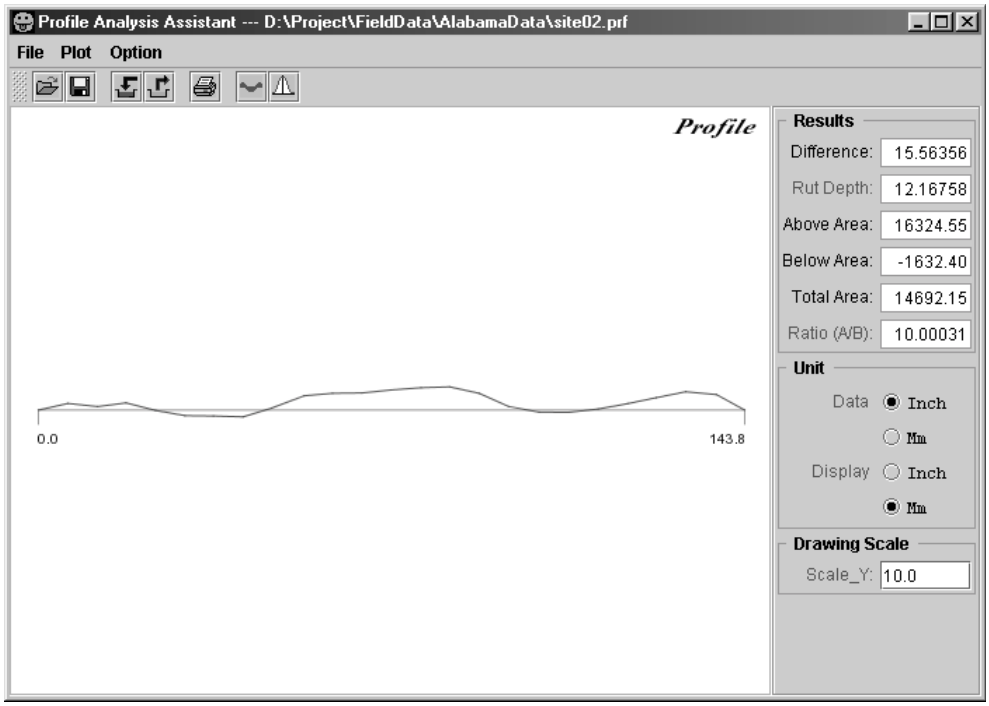

(b) surface profile and distortion parameters

Figure 6-2. Profiles of Alabama Site 2.

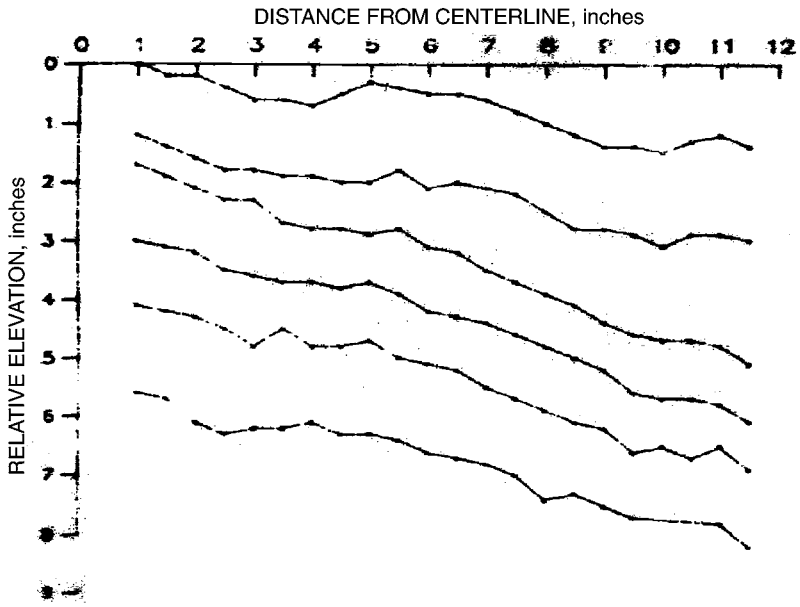

(a) trench profiles

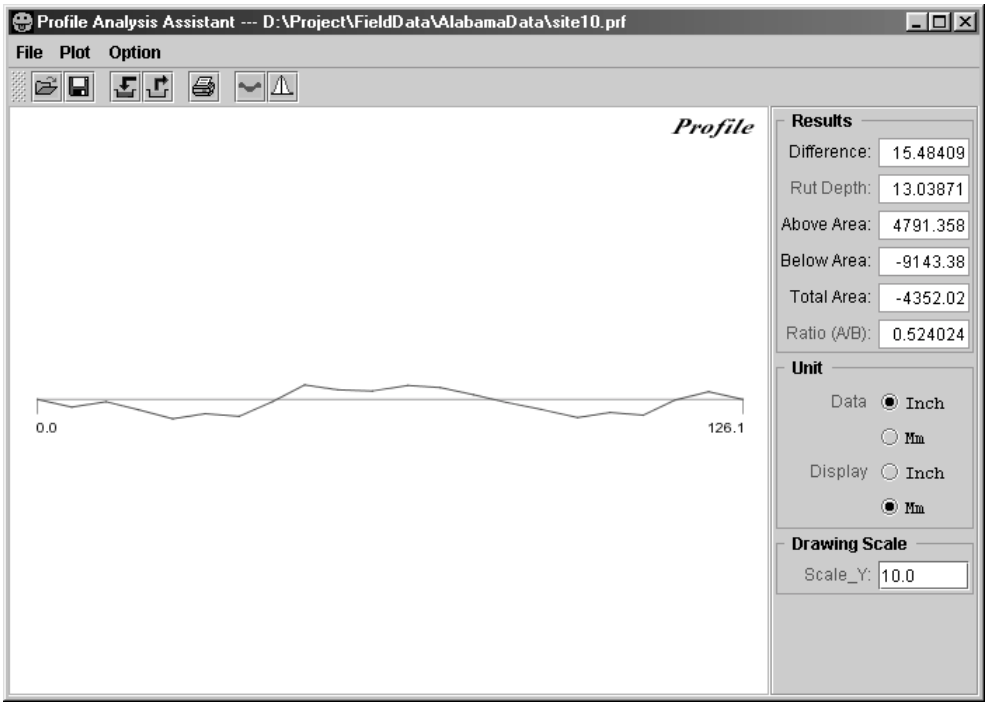

(b) surface profile and distortion parameters

Figure 6-3. Profiles of Alabama Site 10.

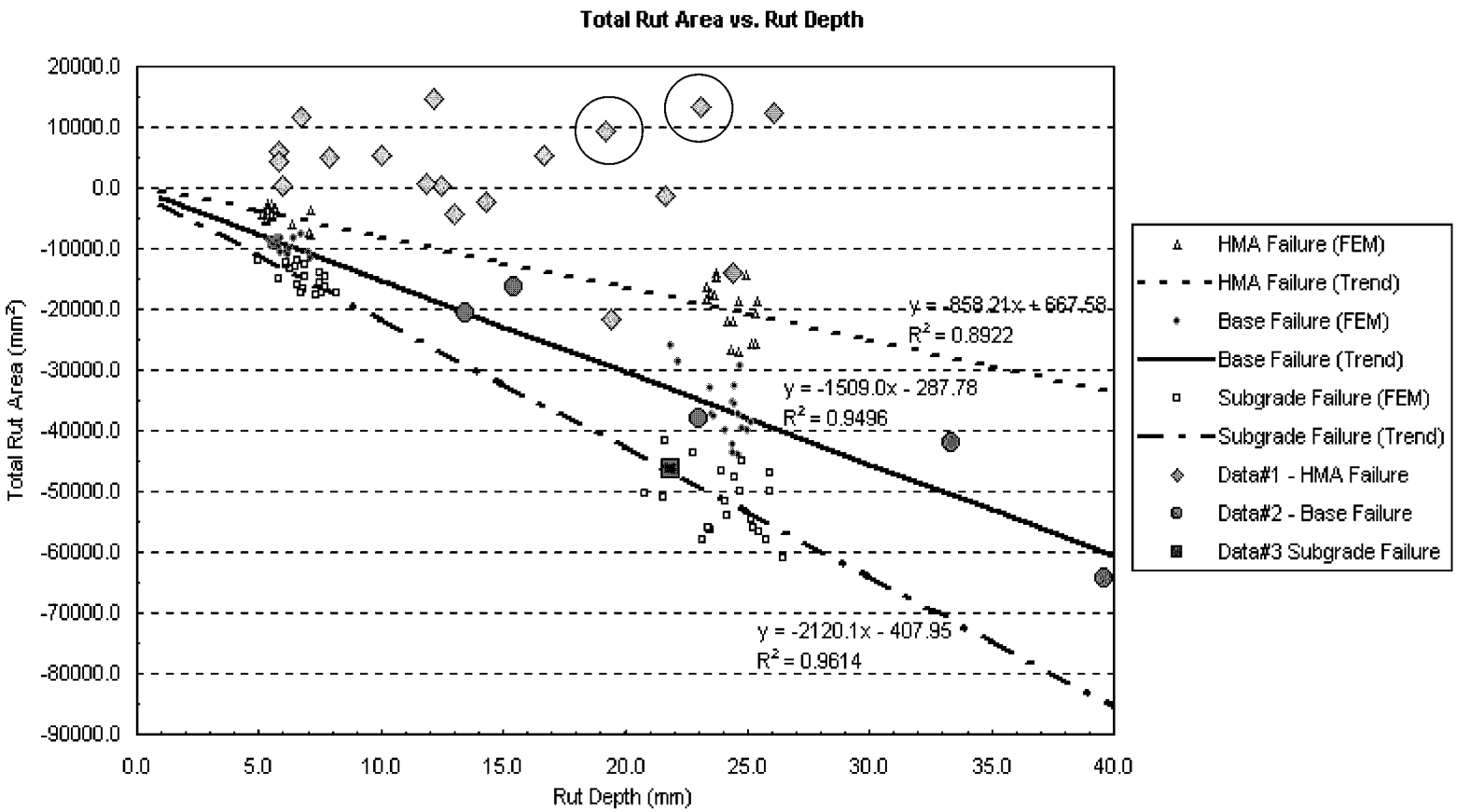

Figure 6-4. Validation of data from Table 6-1.

(a)

(b)

(c)

(d)

(e)

Figure 6-5. Trenching on SH 302 East, Mississippi.

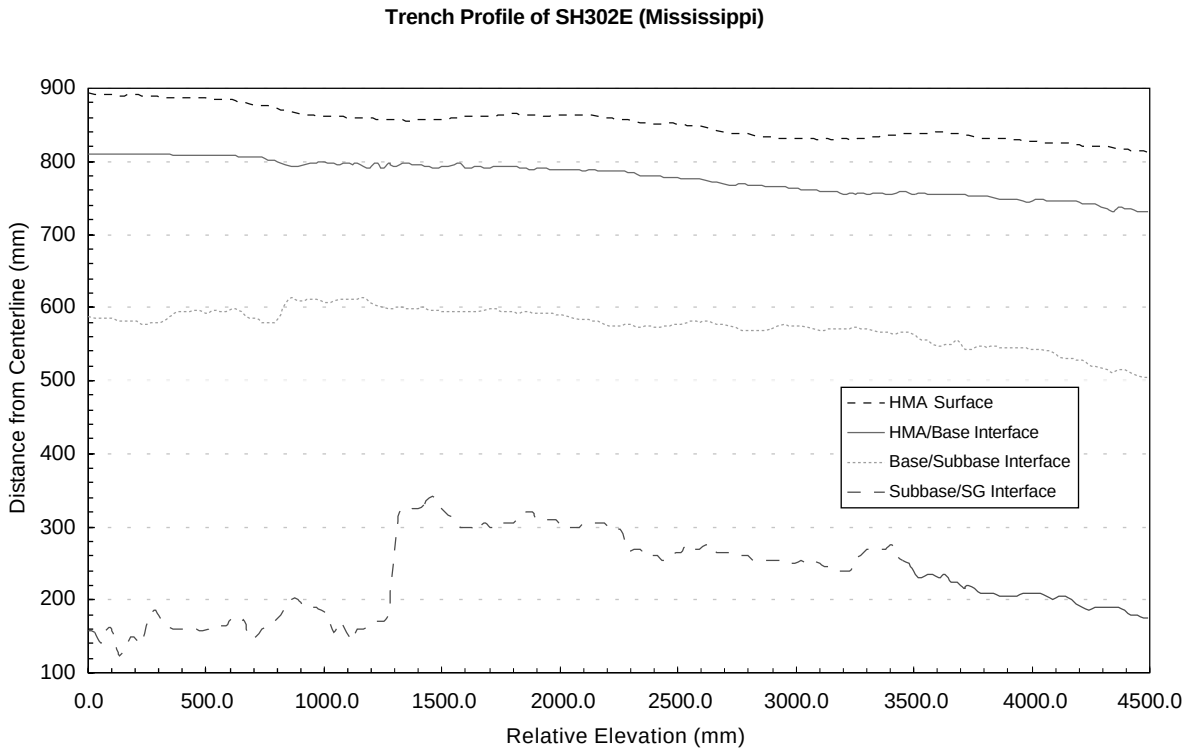

(a) trench profile

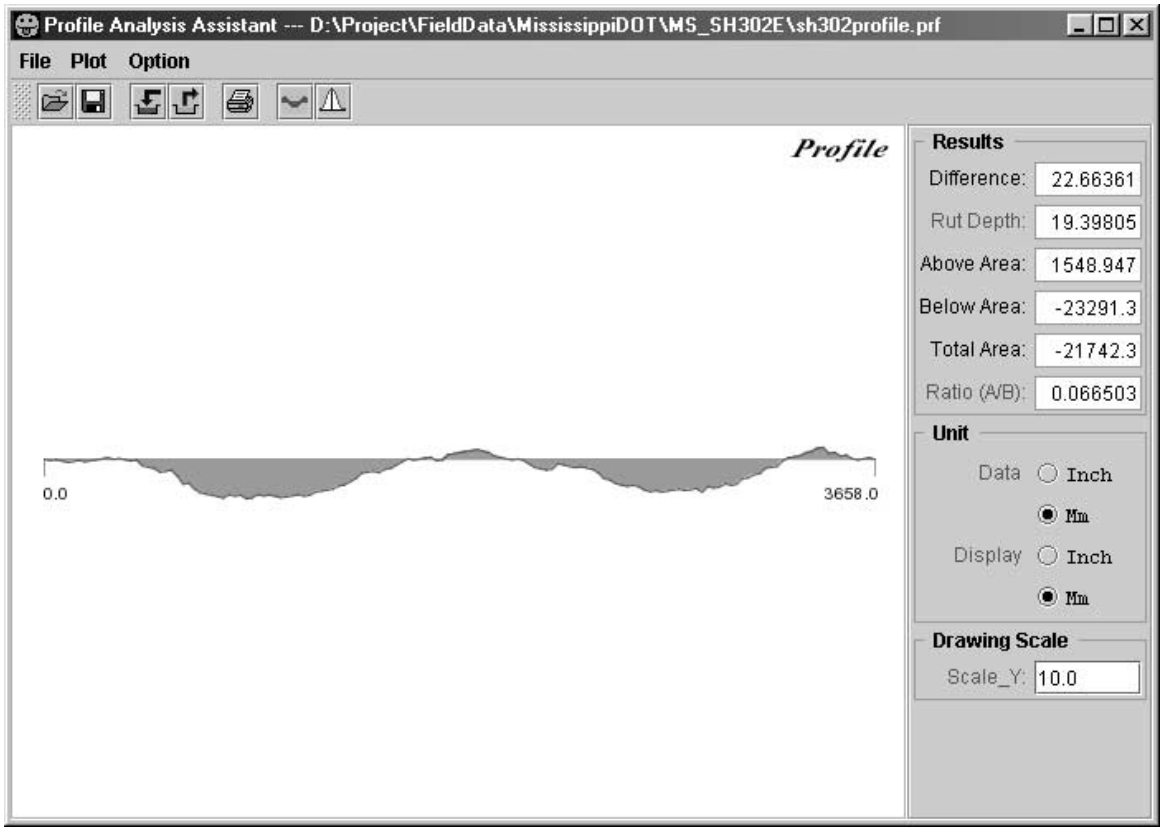

(b) surface profile and distortion parameters

Figure 6-6. Profiles of SH 302 East, Mississippi.

(a)

(d)

(b)

(e)

(c)

(f)

Figure 6-7. Trenching on SH 28 East, Mississippi.

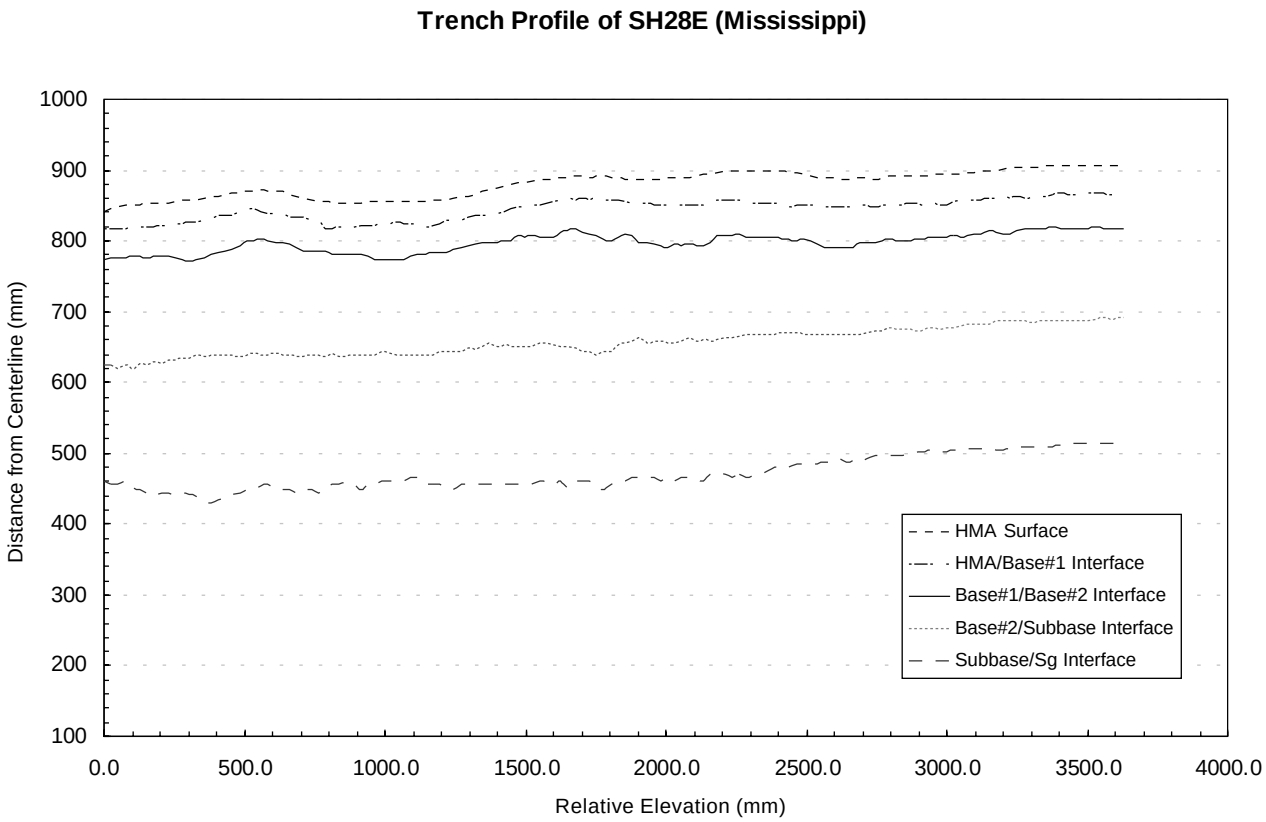

(a) trench profile

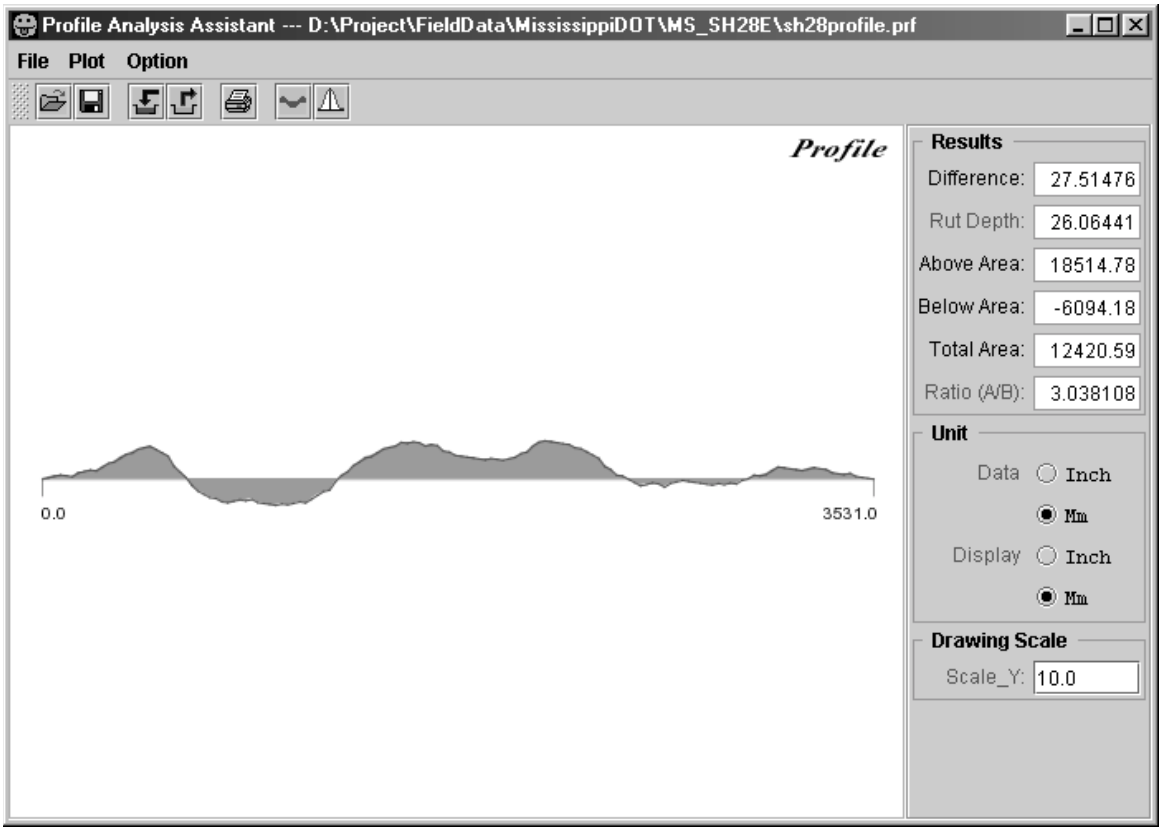

(b) surface profile and distortion parameters

Figure 6-8. Profiles of SH 28 East, Mississippi.

(a)

(b)

Figure 6-9. Trenching on Cell 28, MnROAD.

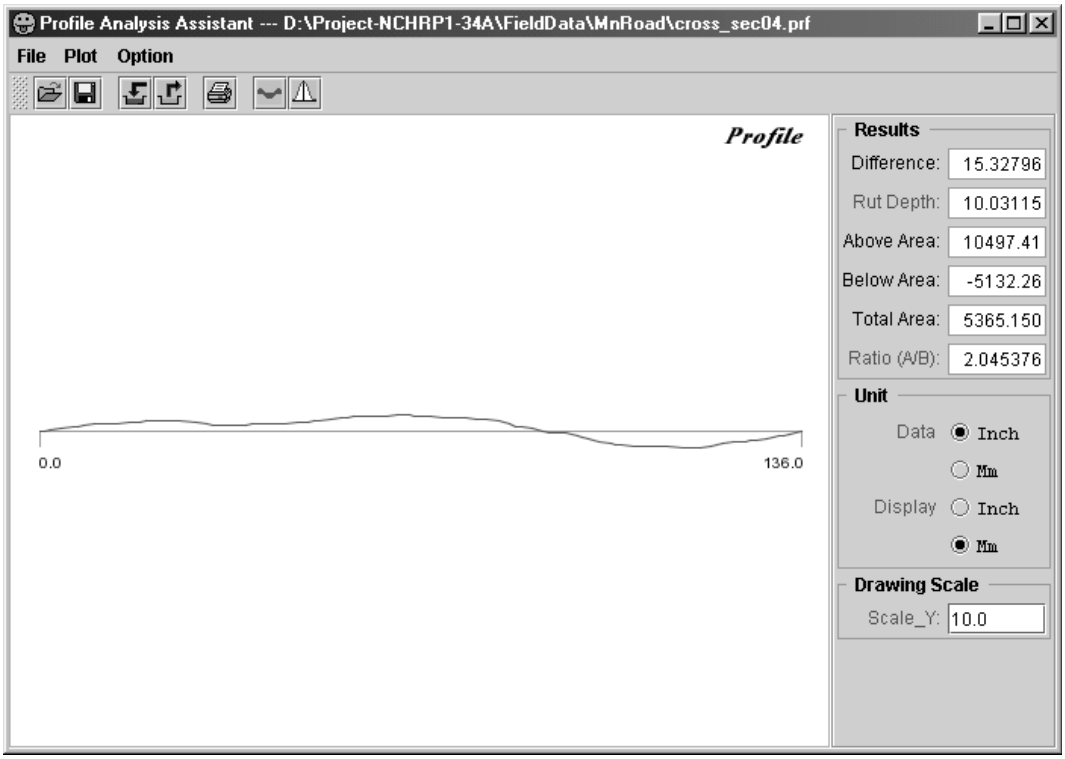

(a) surface profile and distortion parameters

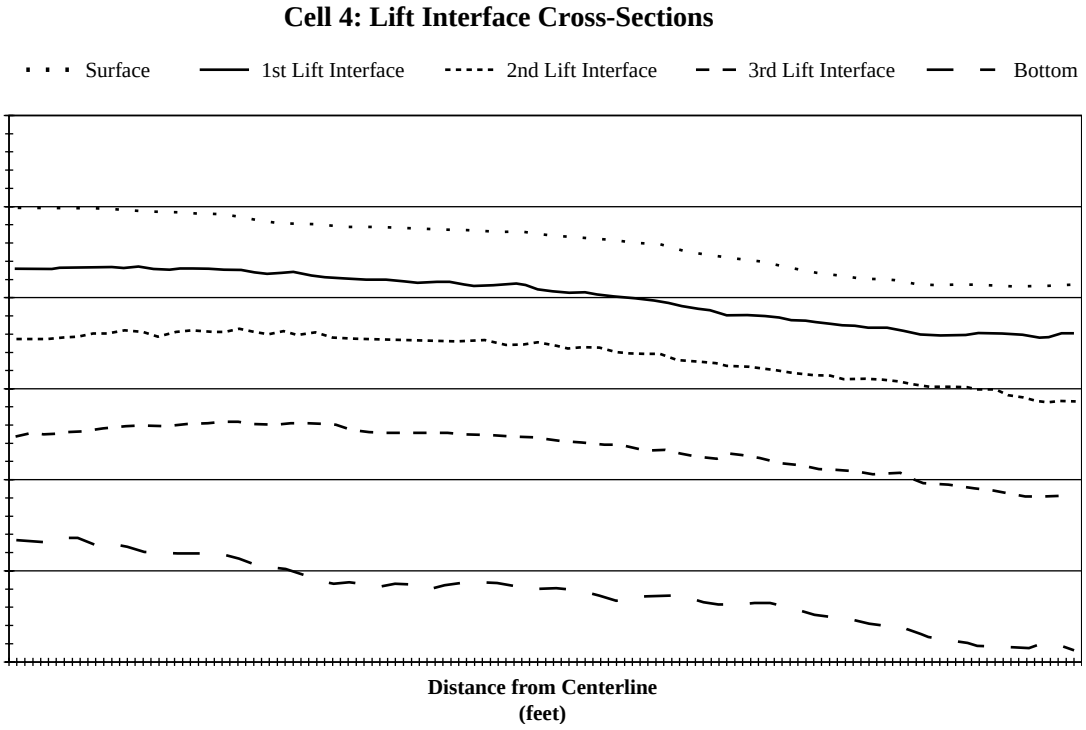

(b) trench profile

Figure 6-10. Profiles of Cell 4.

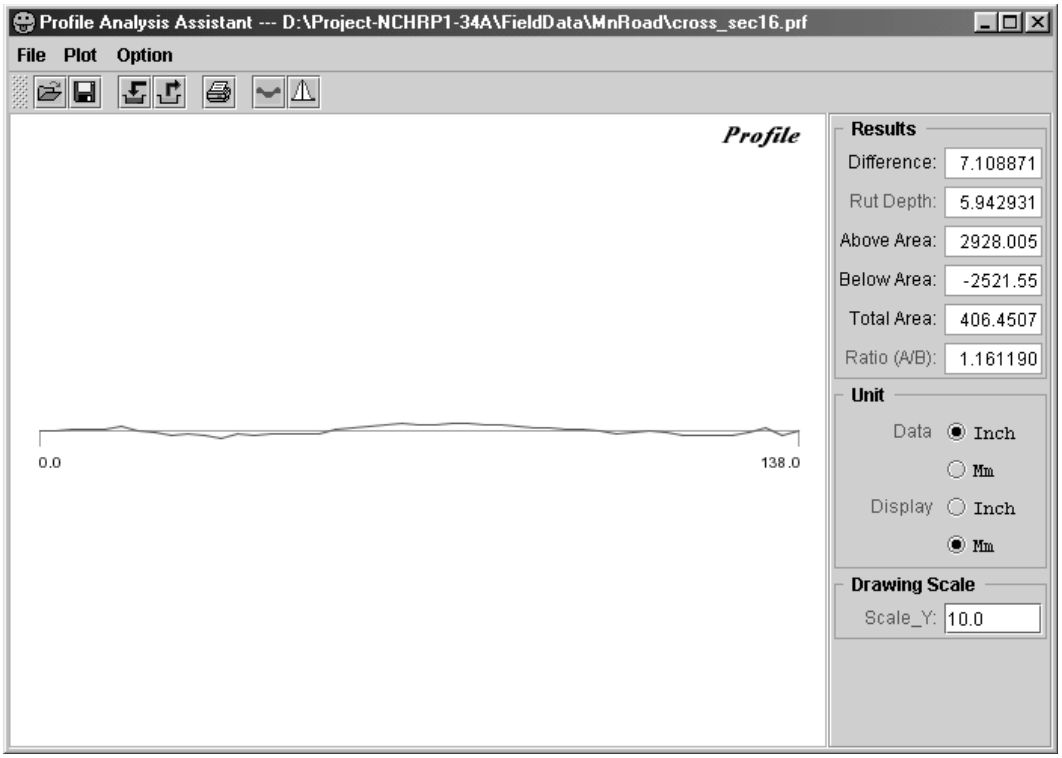

(a) surface profile and distortion parameters

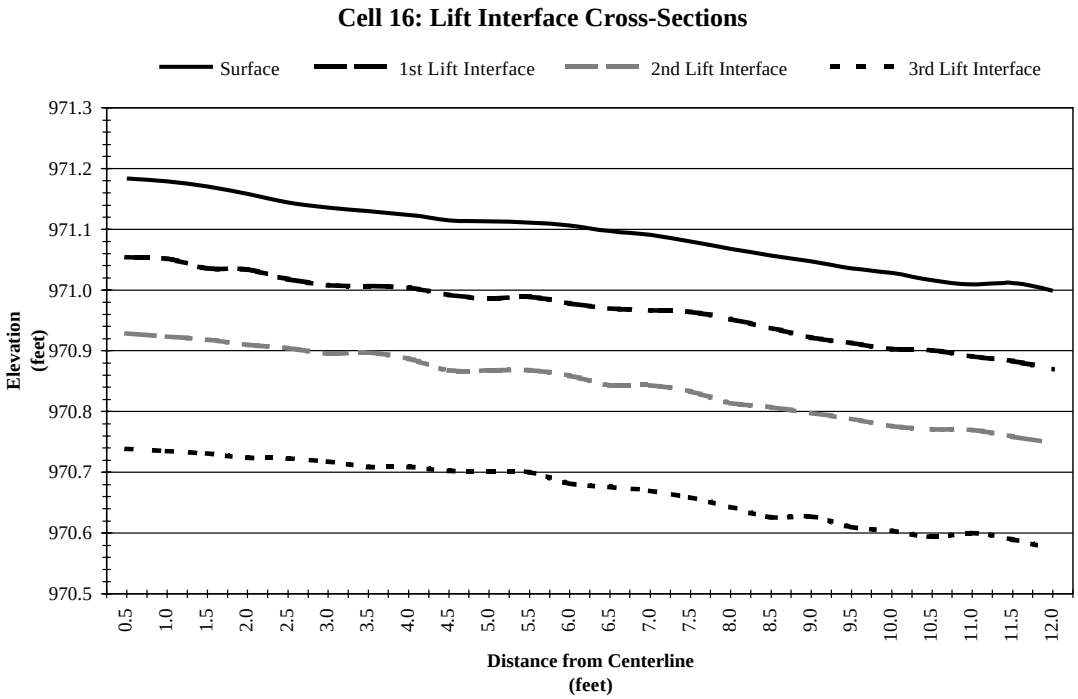

(b) trench profile

Figure 6-11. Profiles of Cell 16.

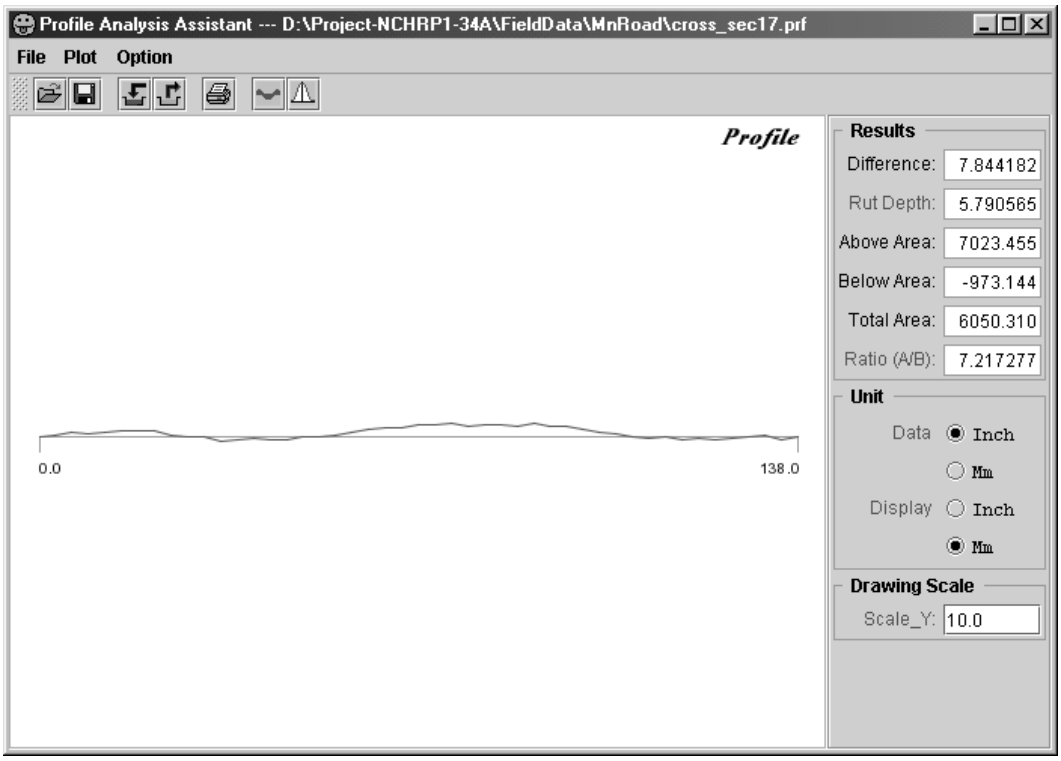

(a) surface profile and distortion parameters

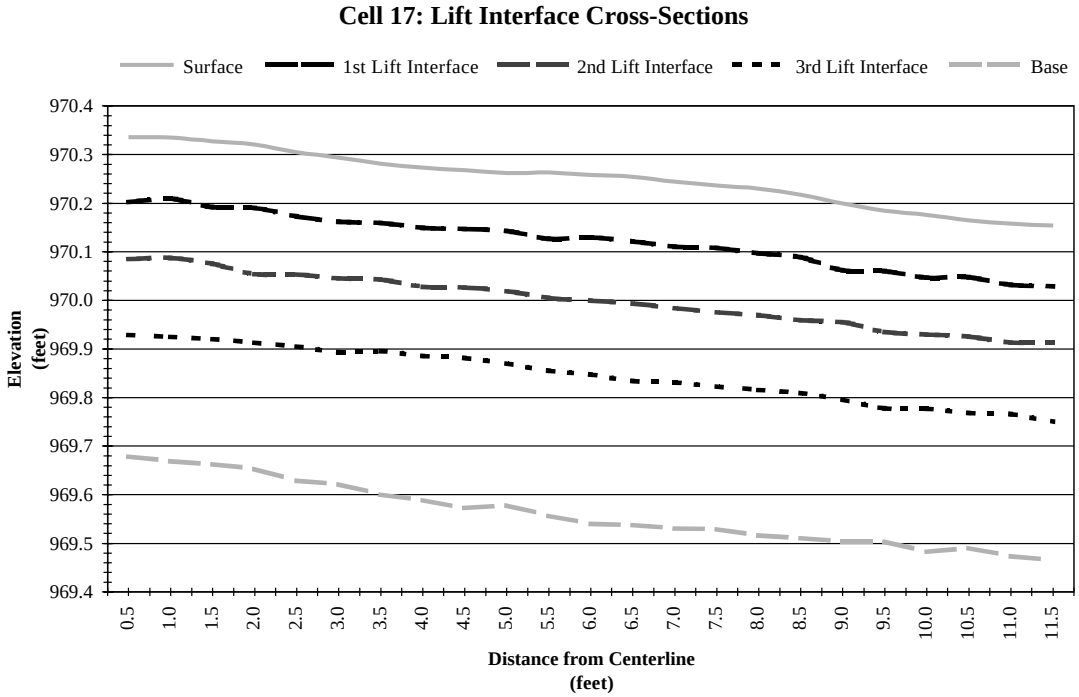

(b) trench profile

Figure 6-12. Profiles of Cell 17.

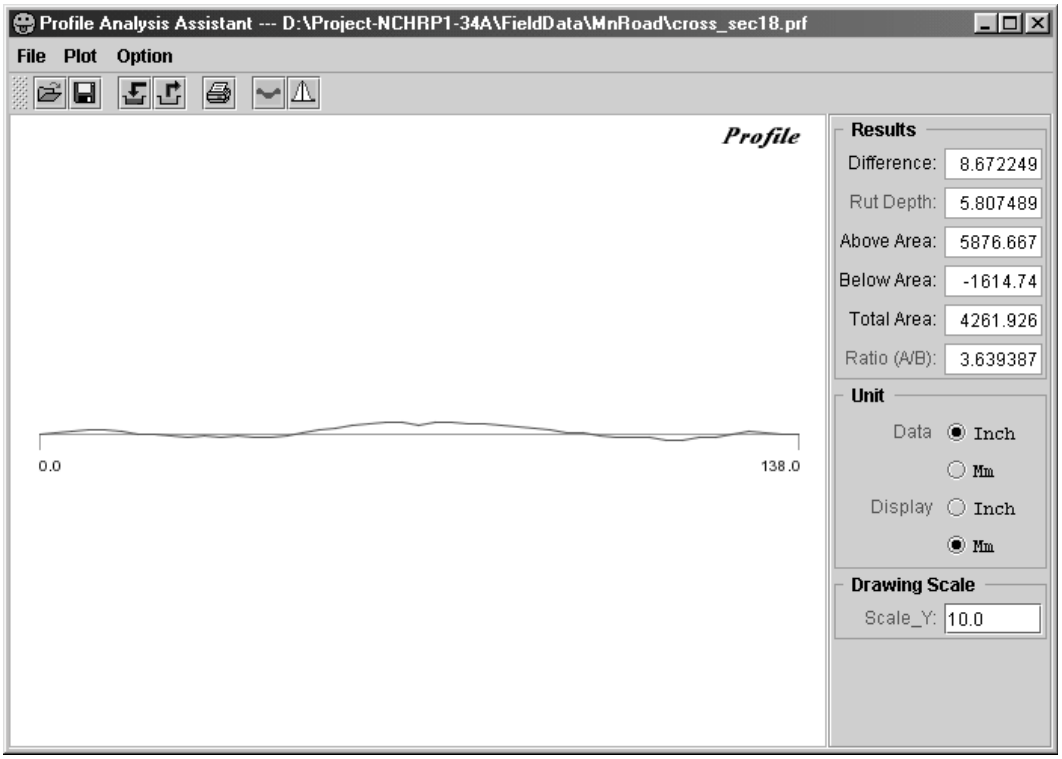

(a) surface profile and distortion parameters

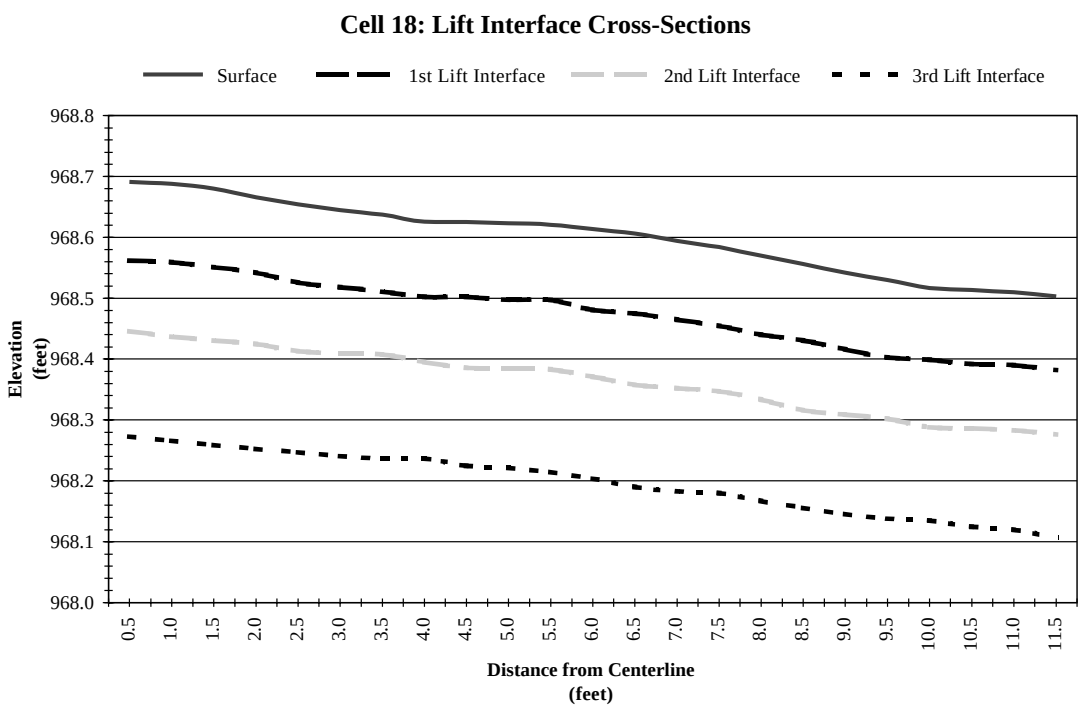

(b) trench profile

Figure 6-13. Profiles of Cell 18.

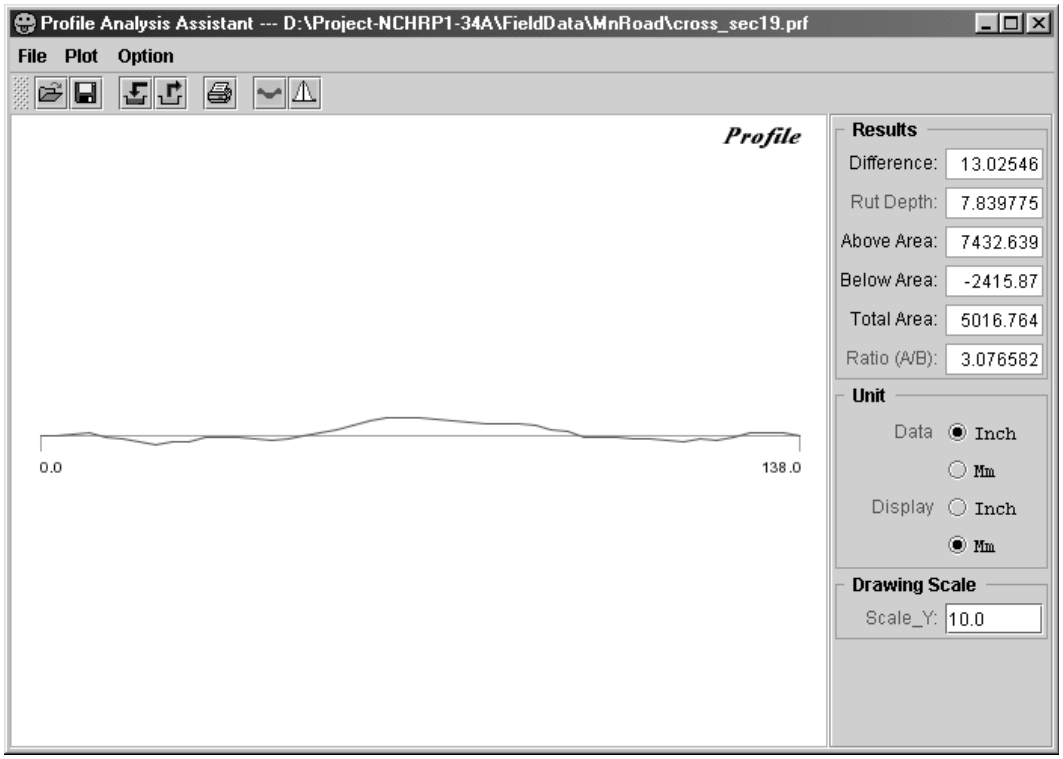

(a) surface profile and distortion parameters

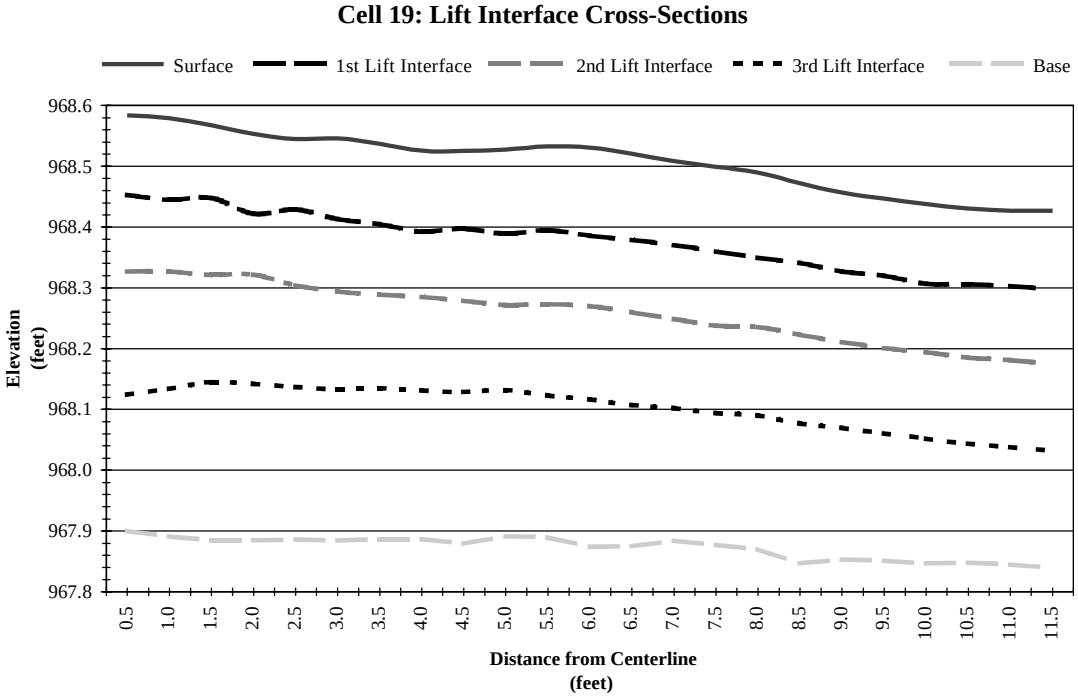

(b) trench profile

Figure 6-14. Profiles of Cell 19.

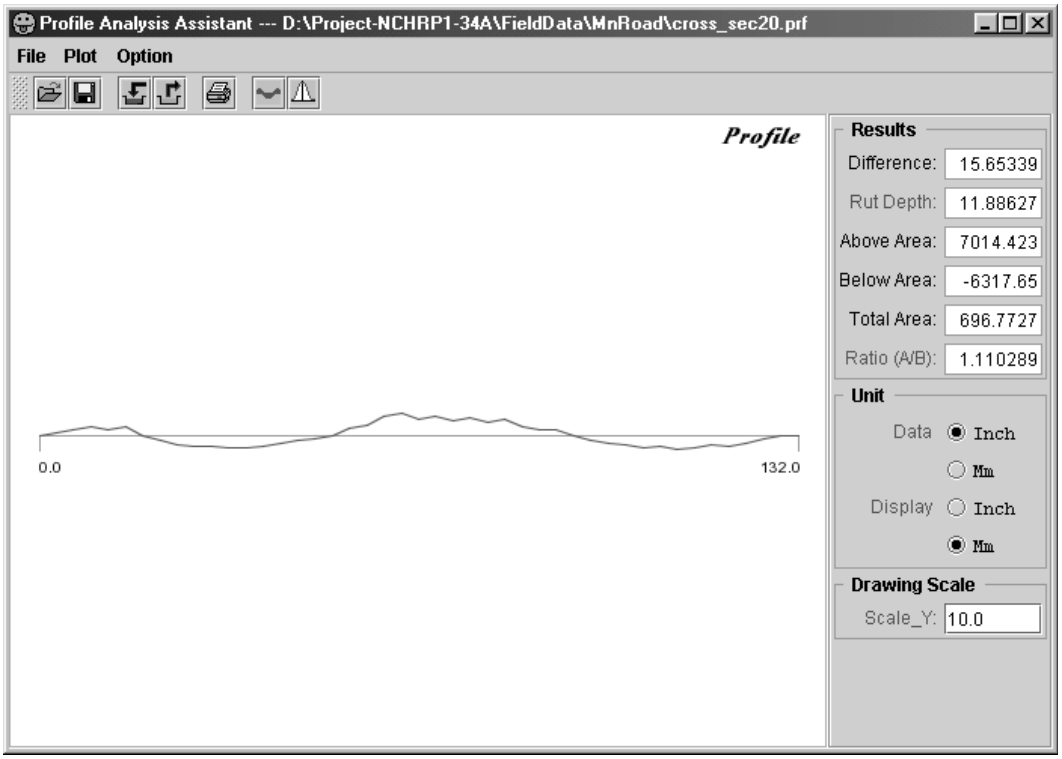

(a) surface profile and distortion parameters

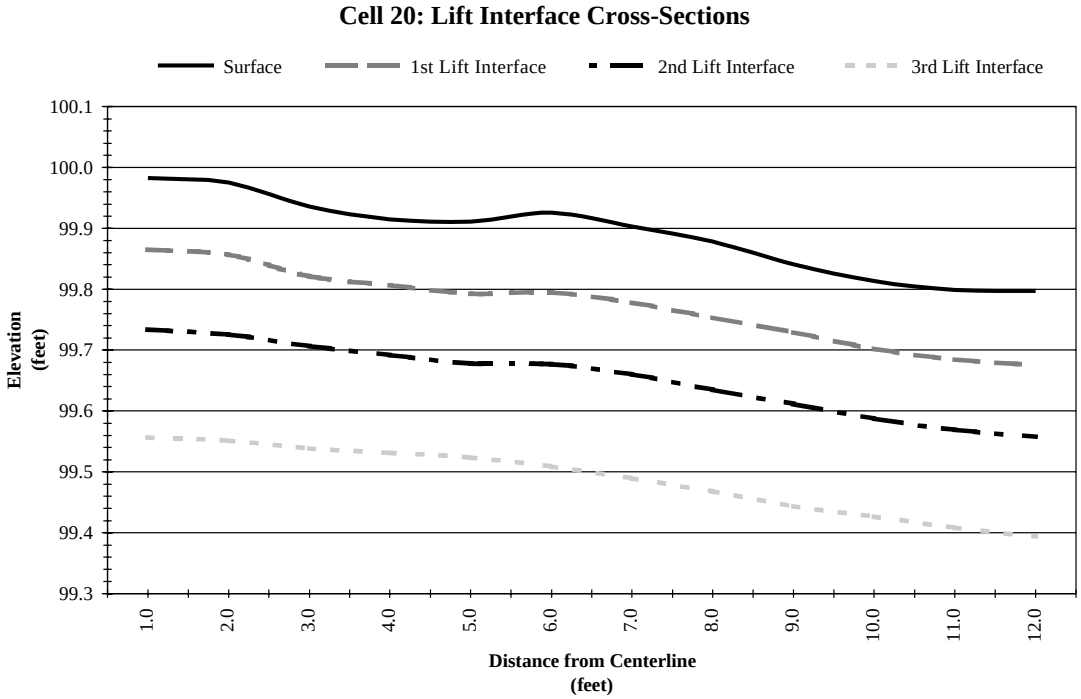

(b) trench profile

Figure 6-15. Profiles of Cell 20.

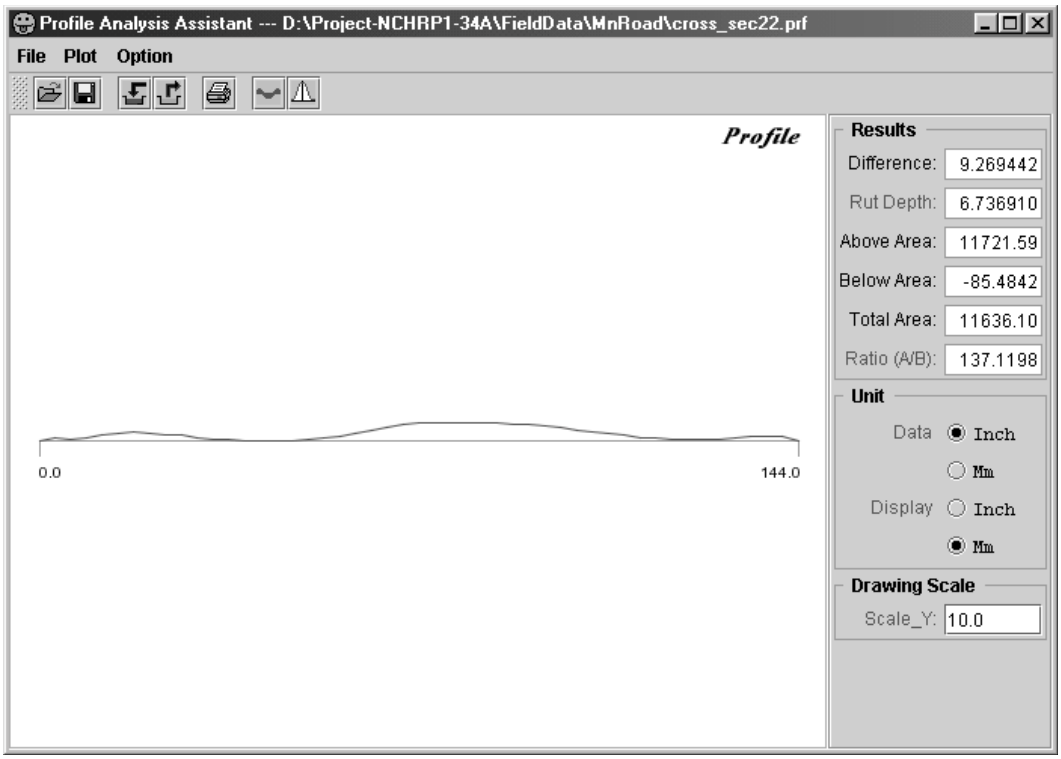

(a) surface profile and distortion parameters

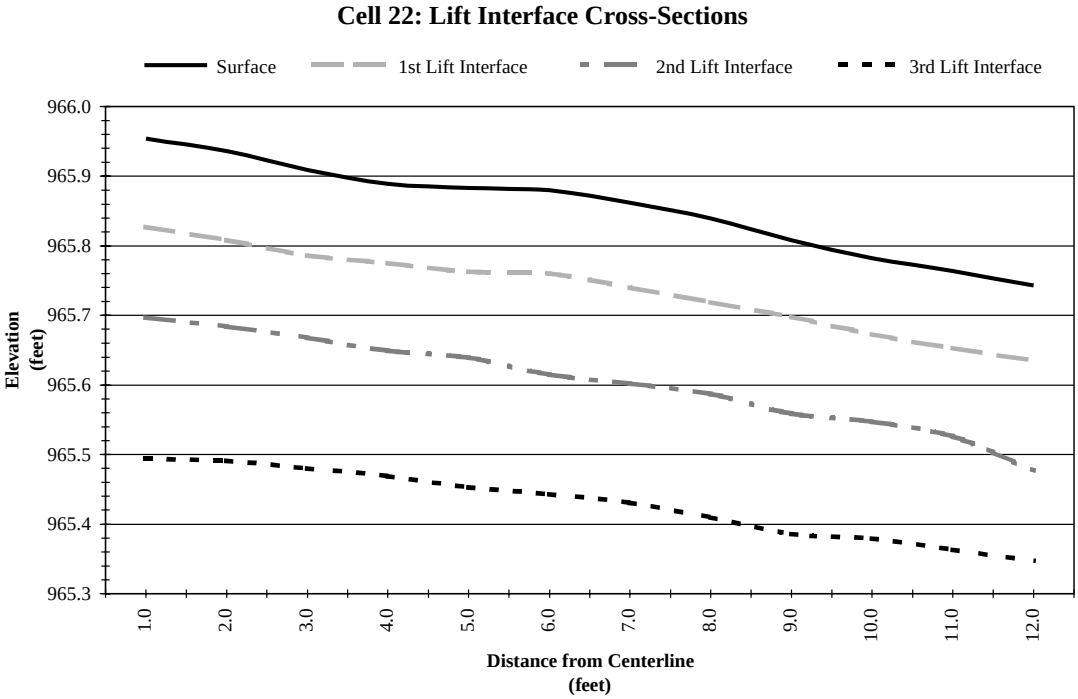

(b) trench profile

Figure 6-16. Profiles of Cell 22.

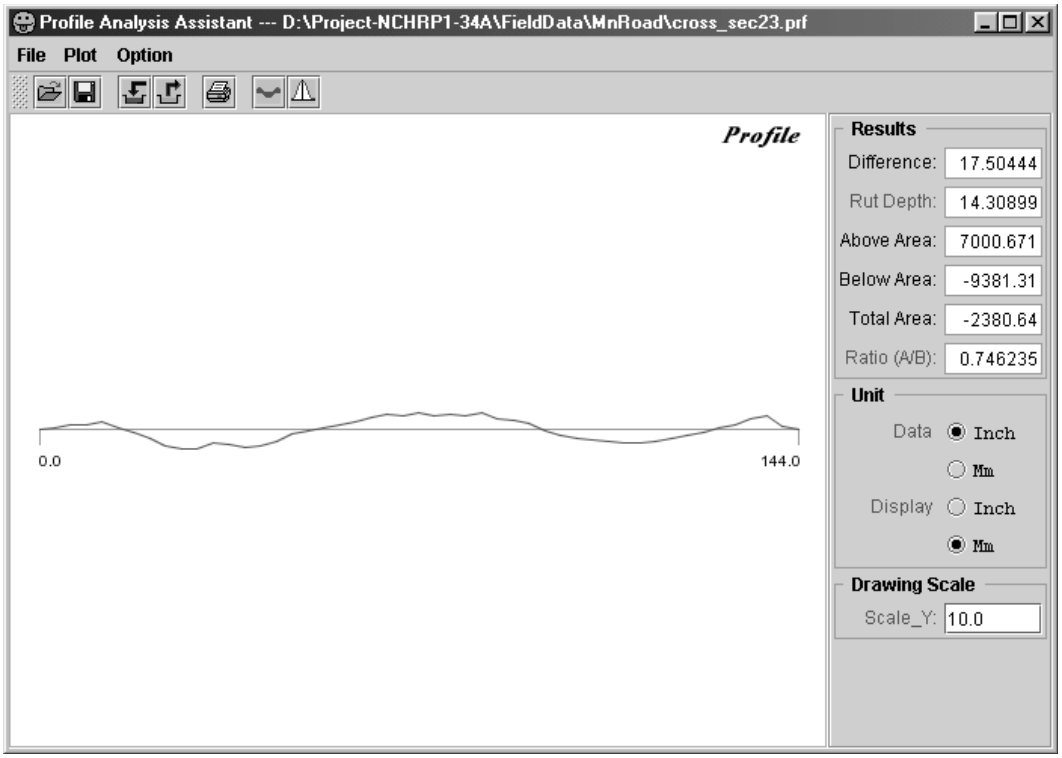

(a) surface profile and distortion parameters

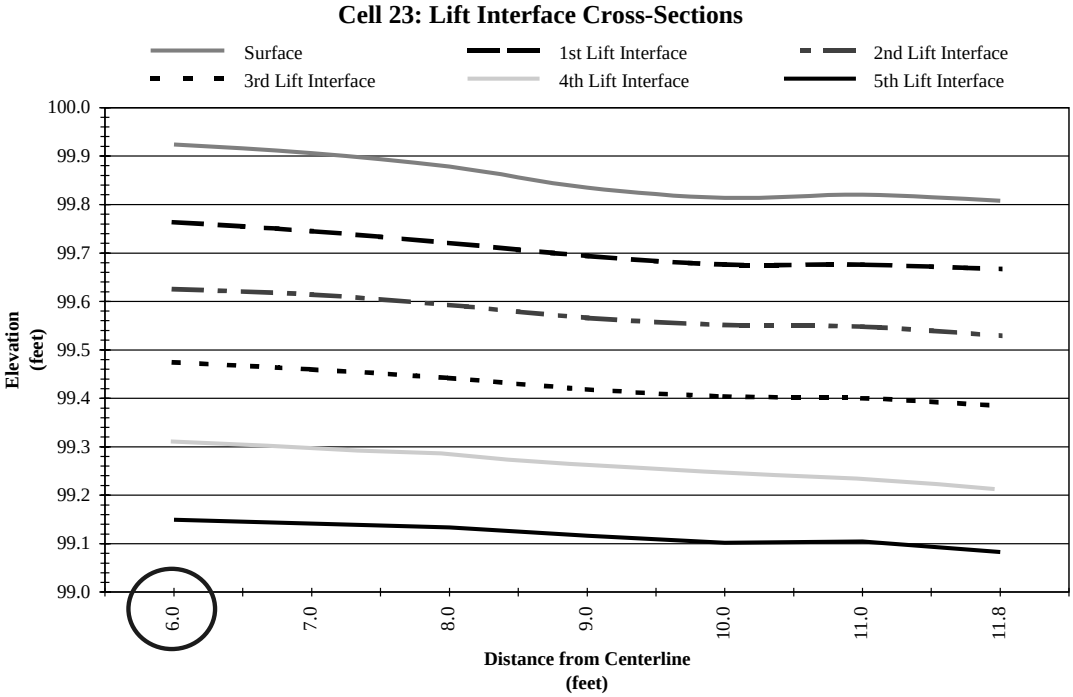

(b) trench profile

Figure 6-17. Profiles of Cell 23.

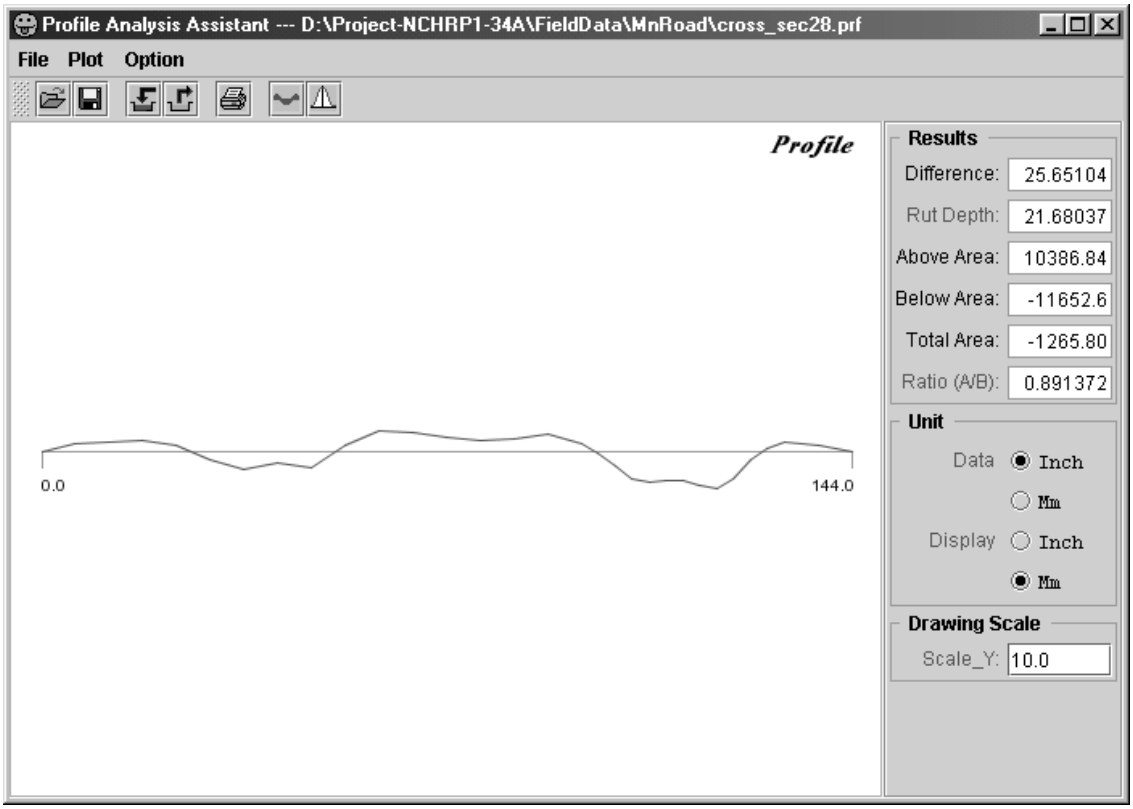

Figure 6-18. Surface profile and distortion parameters of Cell 28.

(a)

(c)

(b)

(d)

Figure 6-19. Trenching on Nevada SR 267.

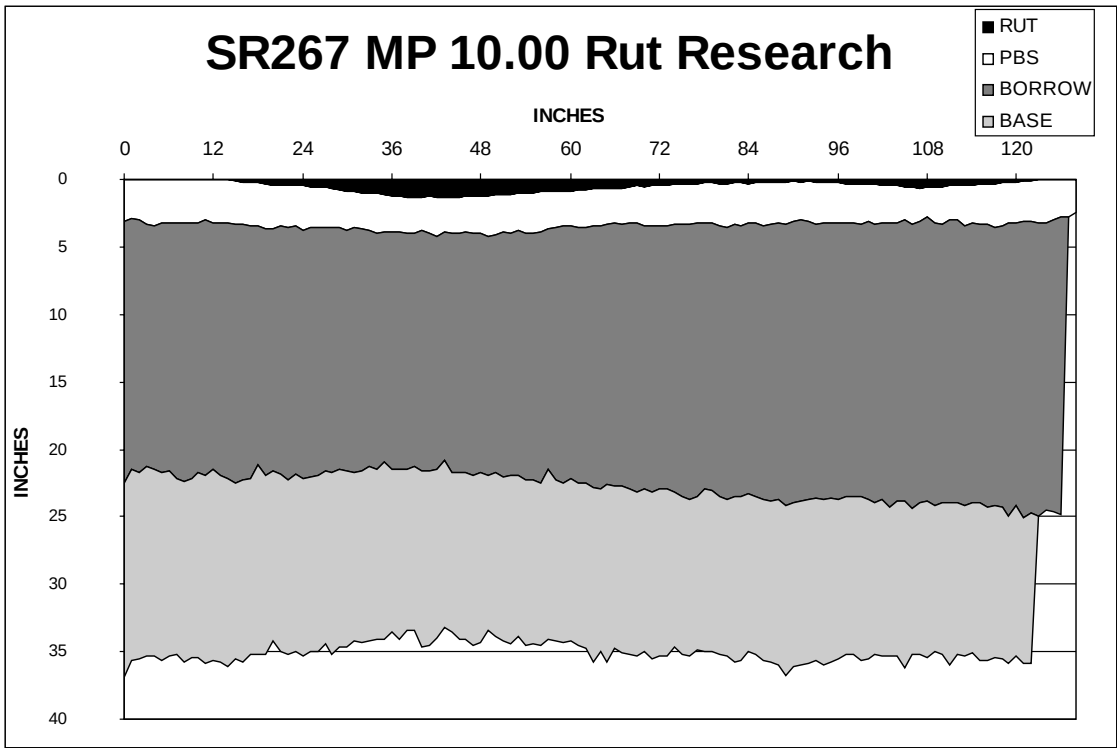

(a) trench profiles

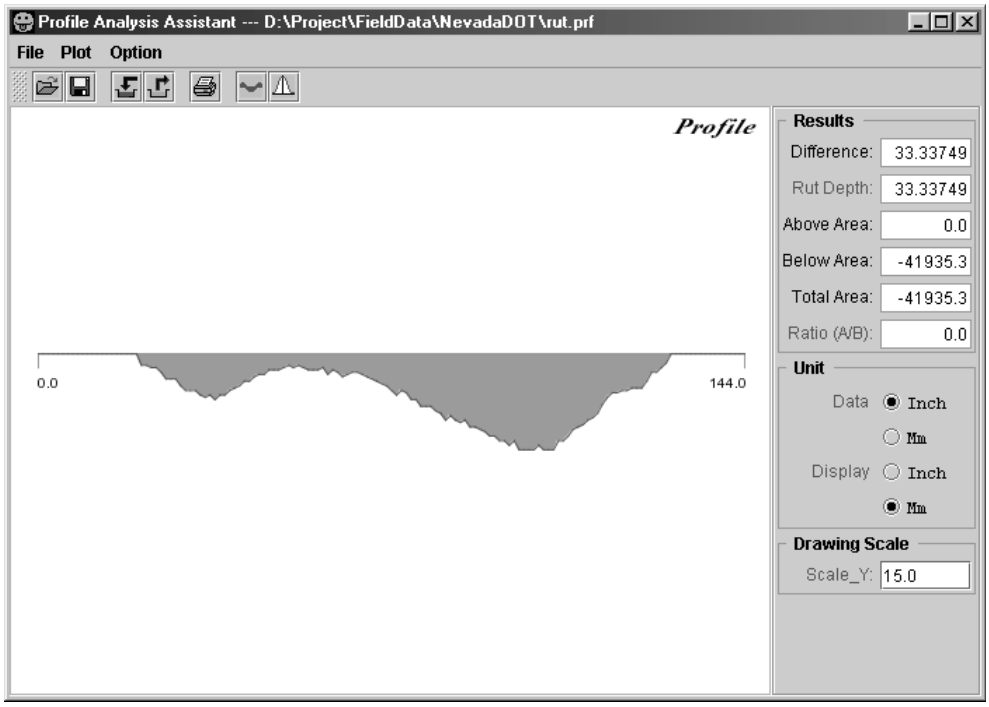

(b) surface profile and distortion parameters

Figure 6-20. Profiles of Nevada SR 267.

(a)

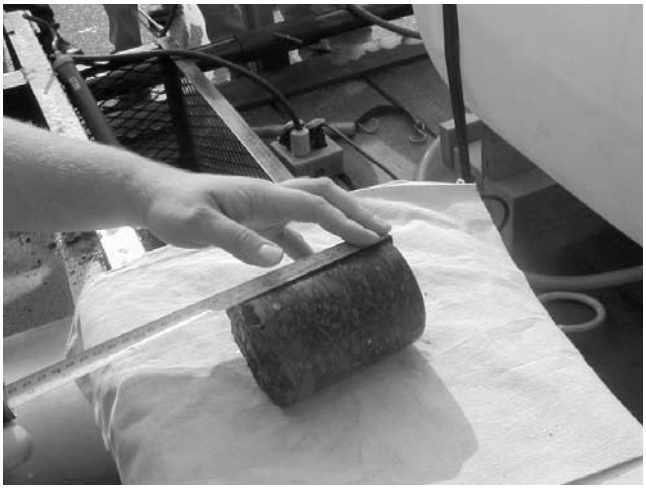

(b)

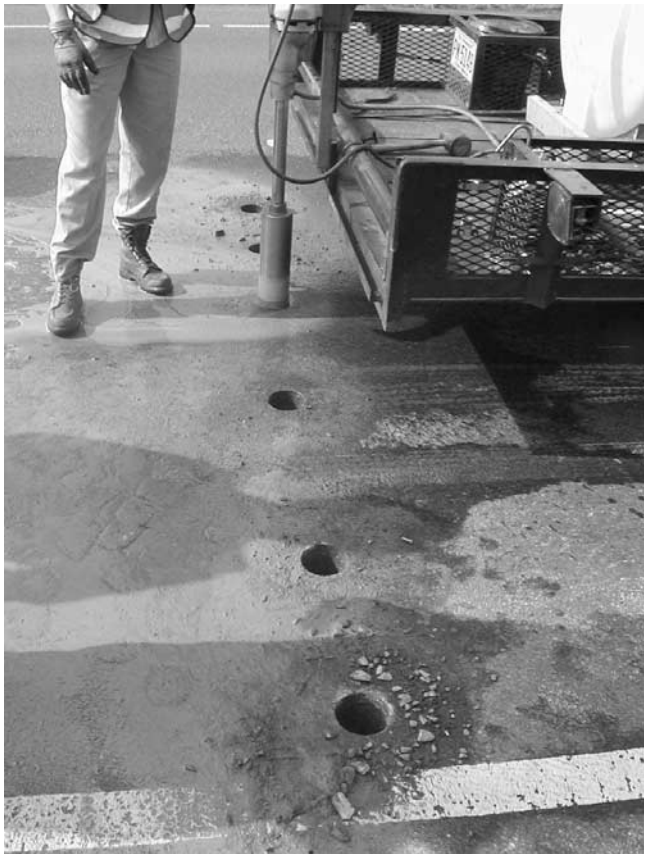

(c)

(d)

Figure 6-21. Trenching on US 64 East, North Carolina.

(e)

(f)

(g)

Figure 6-21 continued.

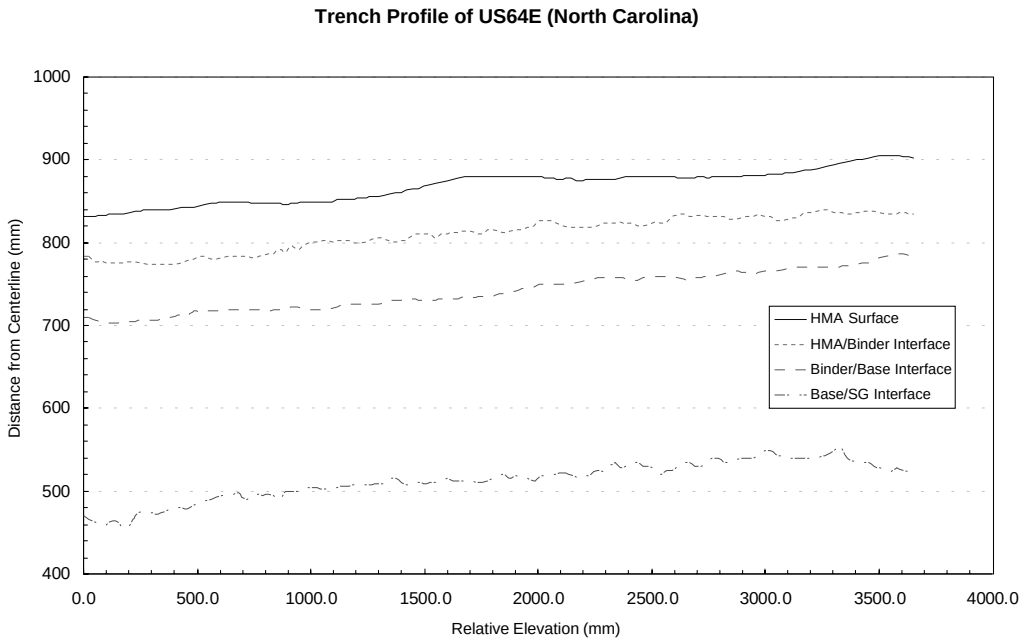

(a) trench profile

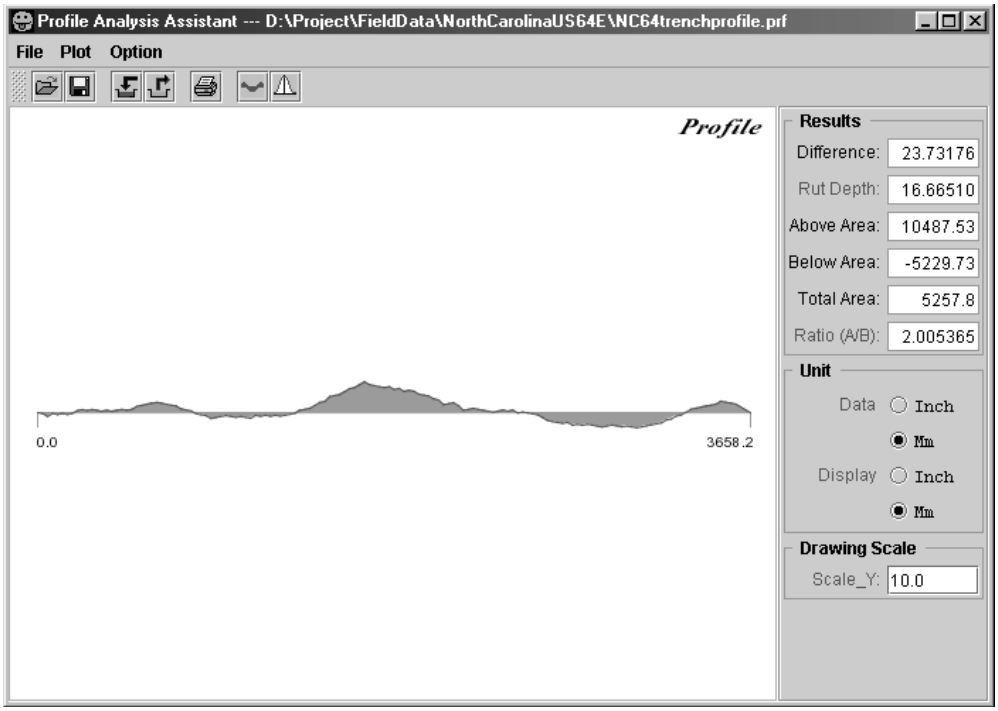

(b) surface profile and distortion parameters

Figure 6-22. Profiles of US 64 East, North Carolina.

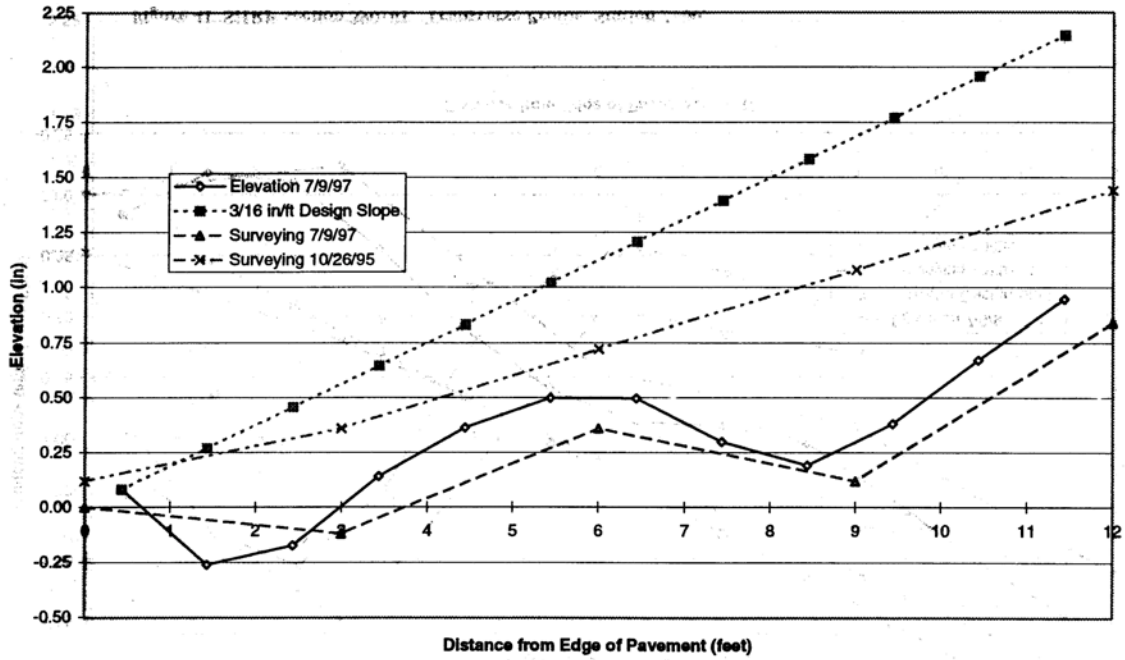

(a) trench profile

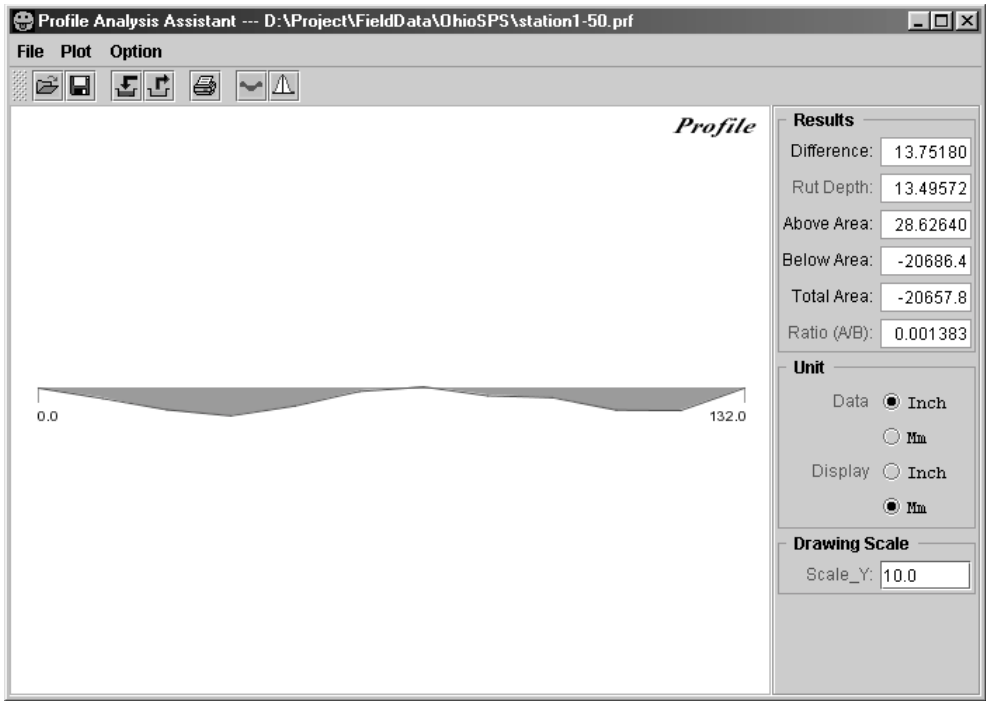

(b) surface profile and distortion parameters

Figure 6-23. Profiles of Ohio SPS-1 Project, Site 390101, Station 1 + 50.

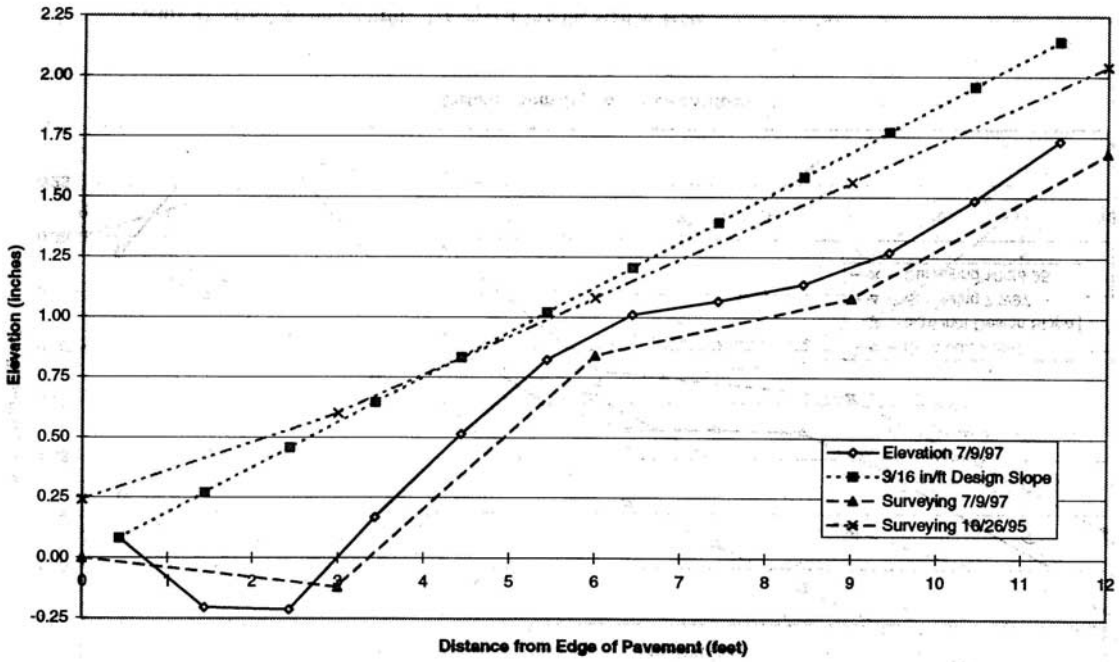

(a) trench profile

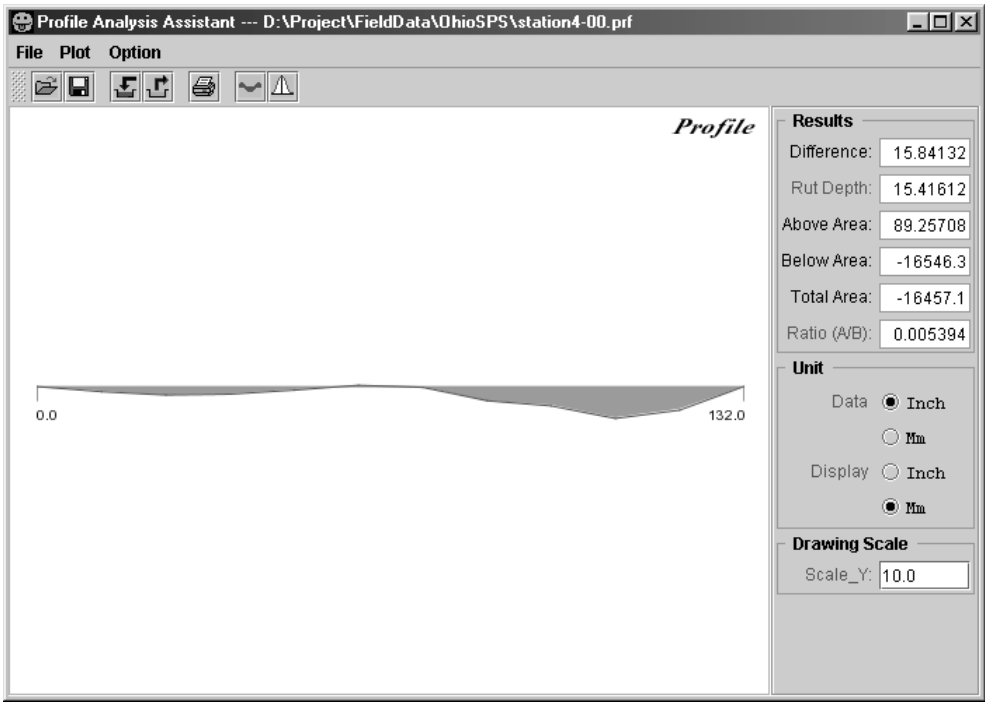

(b) surface profile and distortion parameters

Figure 6-24. Profiles of Ohio SPS-1 Project, Site 390101, Station 4 + 00.

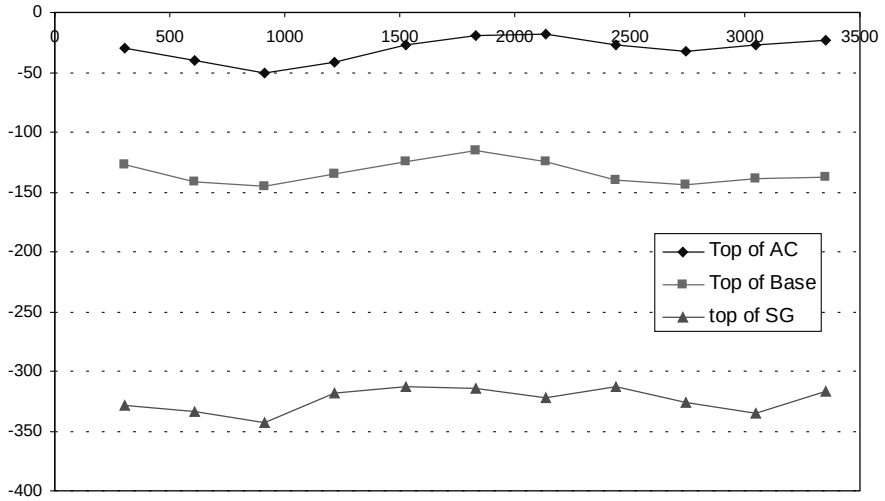

(a) trench profile

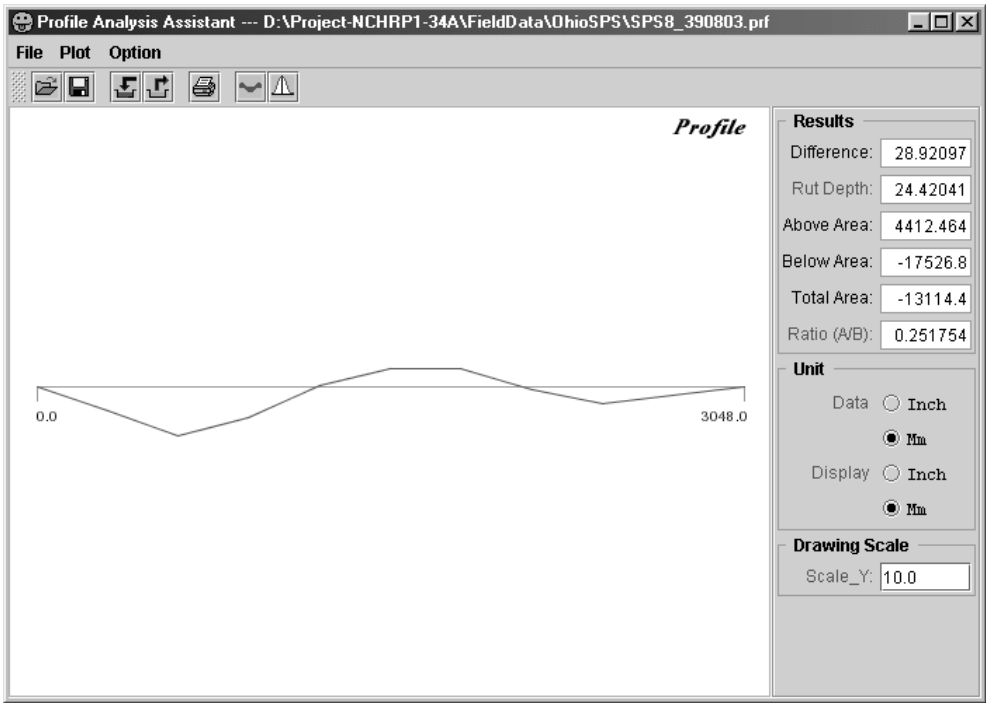

(b) surface profile and distortion parameters

Figure 6-25. Profiles of Ohio SPS-8 Project, Site 390803.

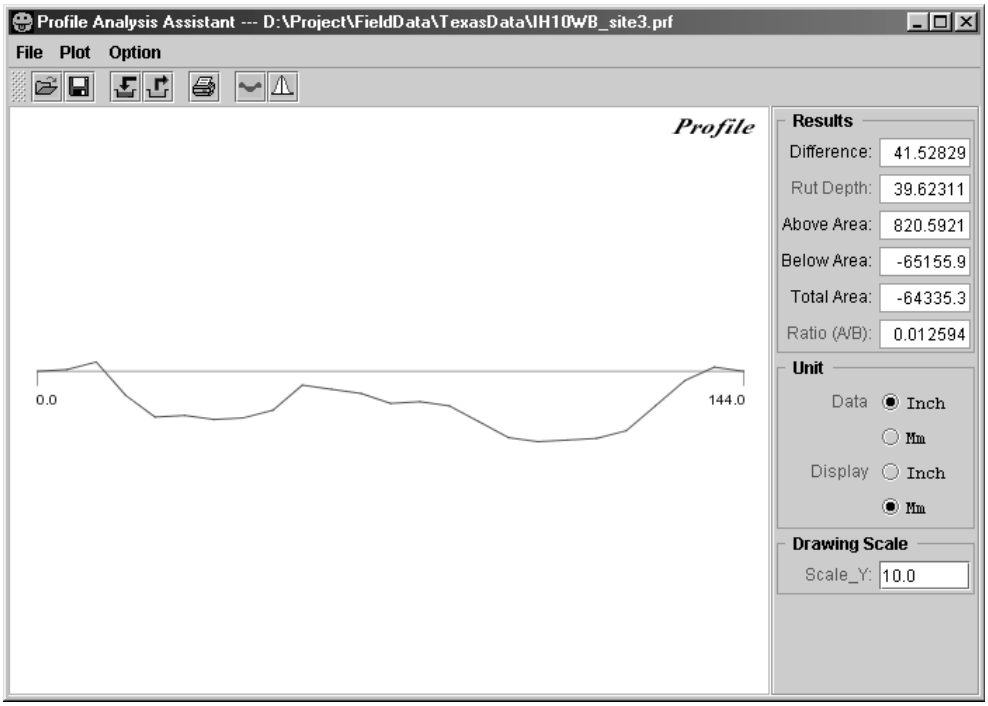

Figure 6-26. Surface profile and distortion parameters of Texas IH 10WB, Site 3.

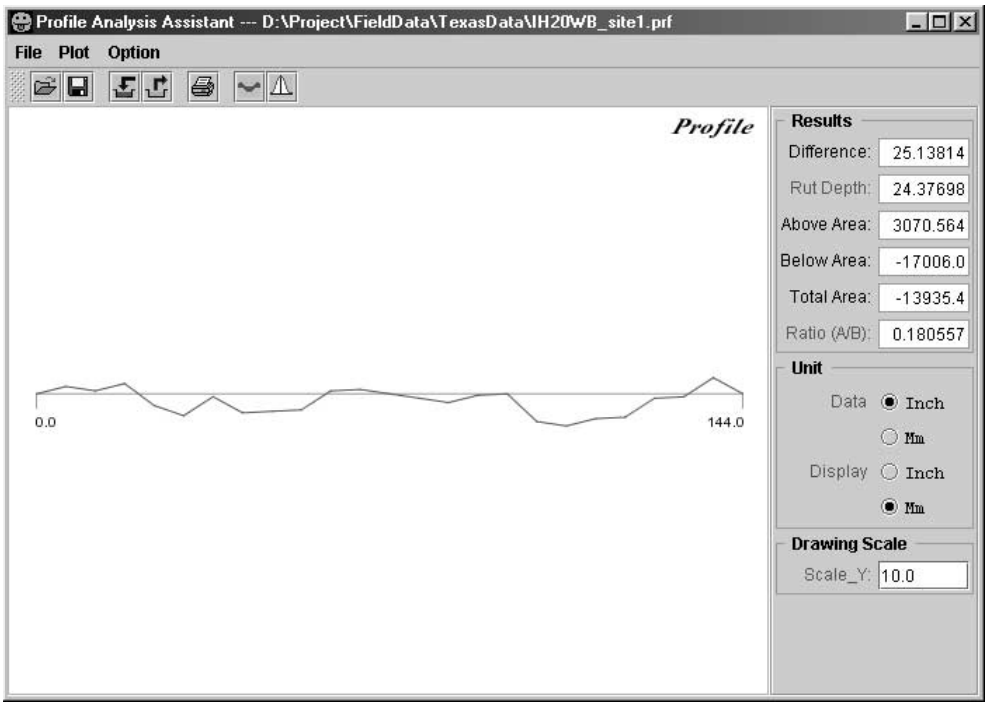

Figure 6-27. Surface profile and distortion parameters of Texas IH 20WB, Site 1.

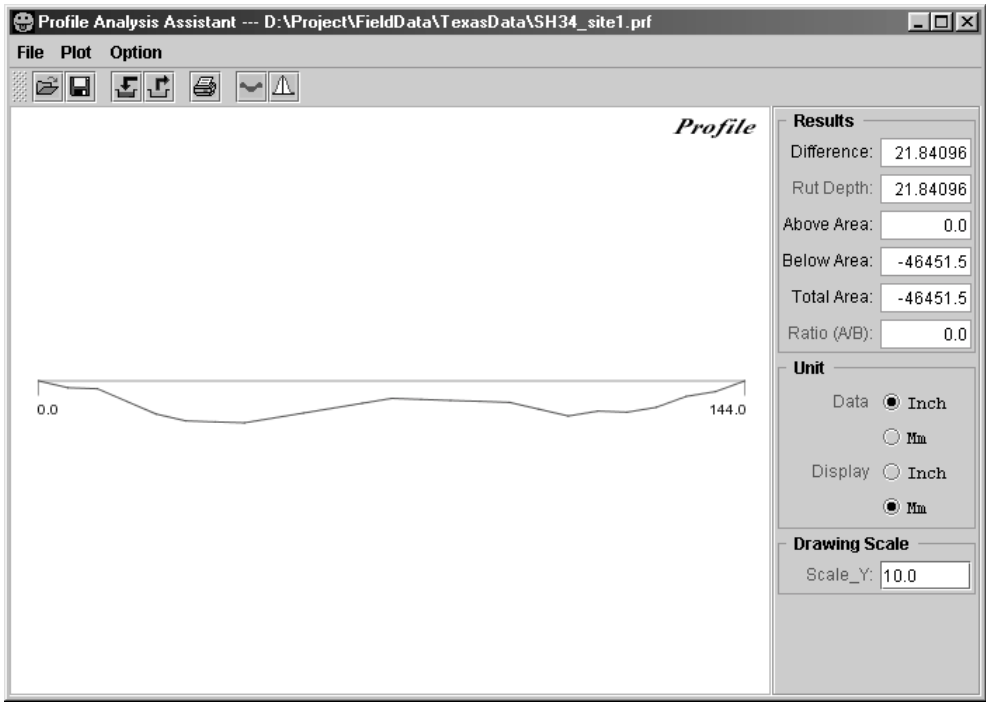

Figure 6-28. Surface profile and distortion parameters of Texas SH 34, Site 1.

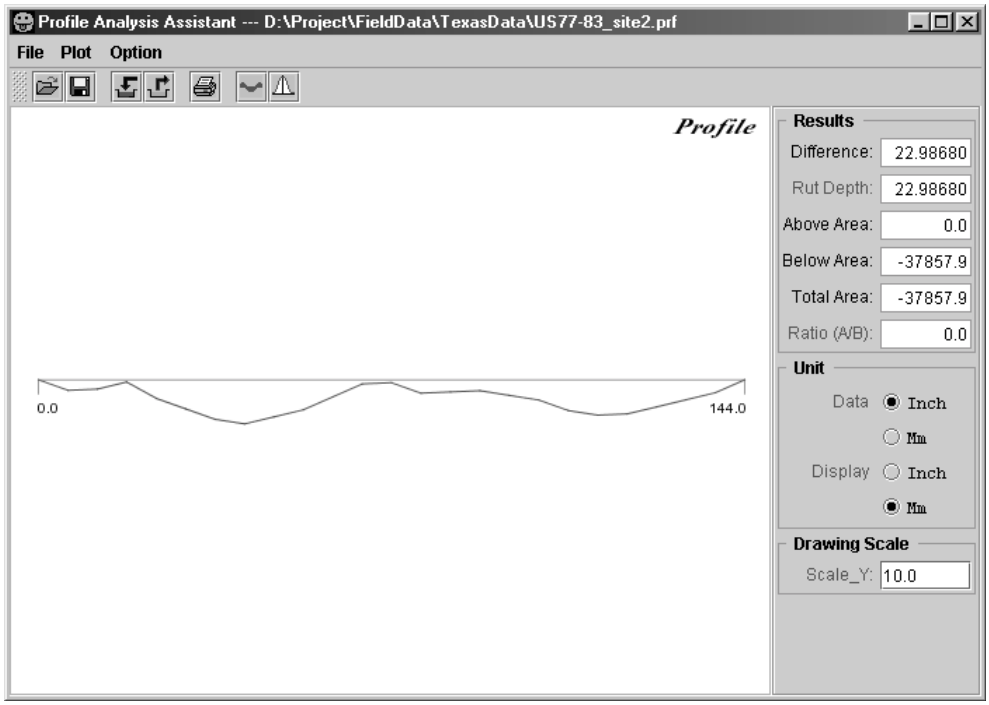

Figure 6-29. Surface profile and distortion parameters of Texas US 77-83, Site 2.

(a)

(c)

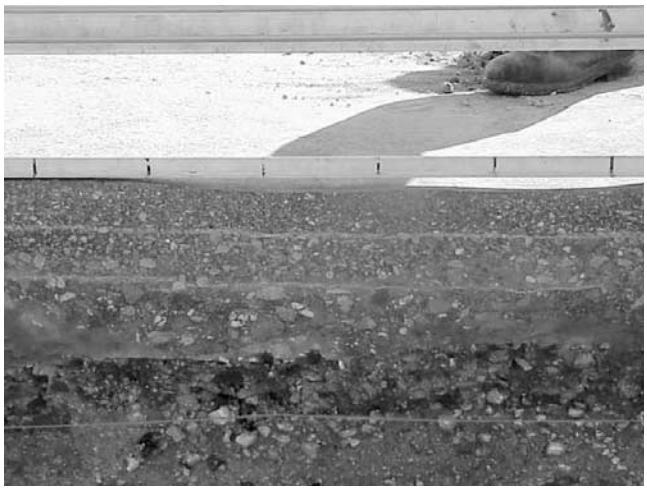

(b)

(d)

Figure 6-30. Trenching on Section 480161, US 281, Texas.

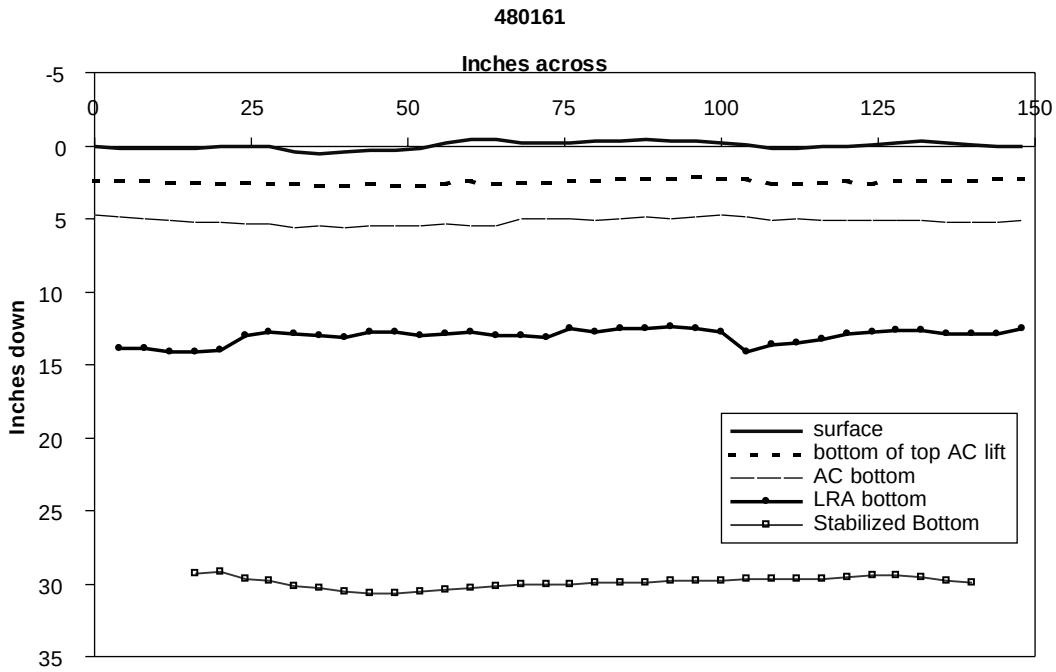

(a) trench profile

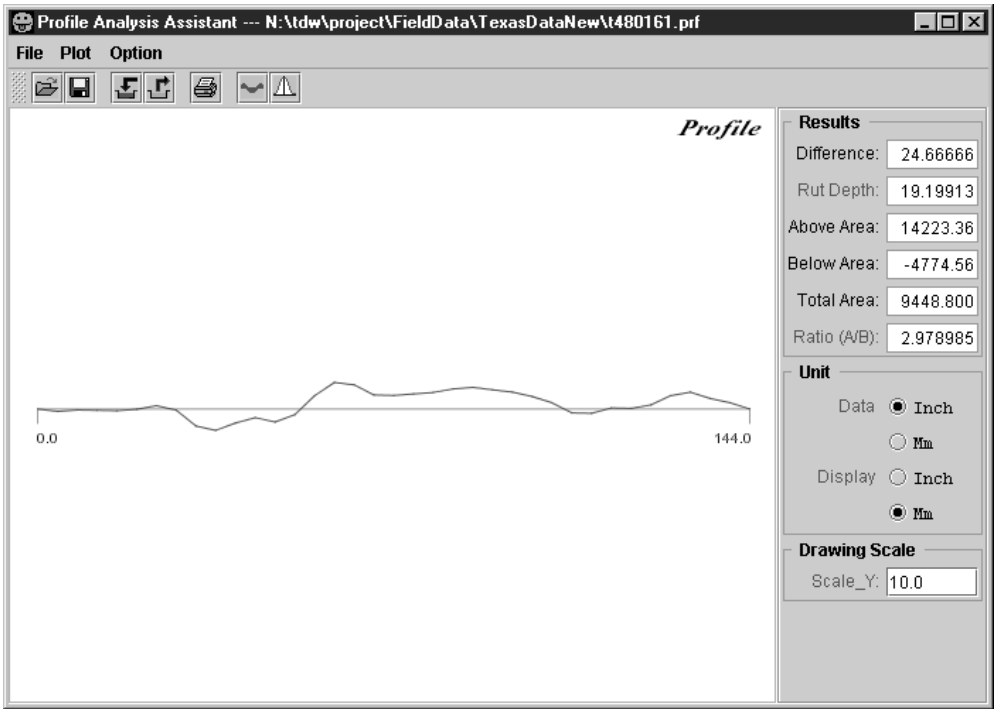

(b) surface profile and distortion parameters.

Figure 6-31. Profiles of Section 480161, US 281, Texas.

(a)

(c)

(b)

(d)

Figure 6-32. Trenching on Section 480162, US 281, Texas.

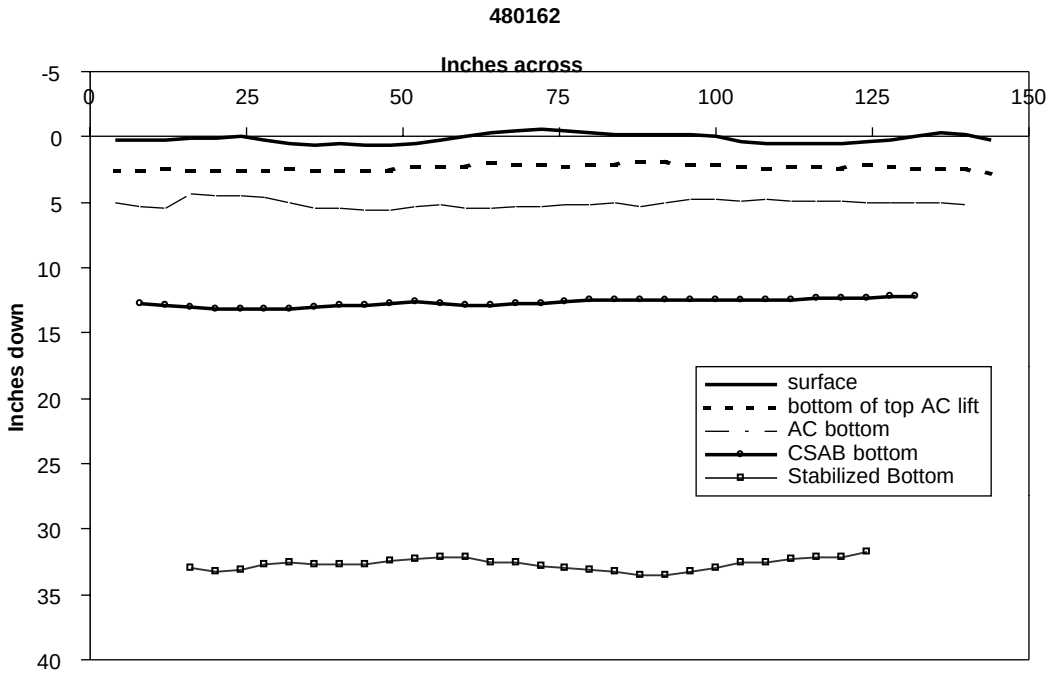

(a) trench profile

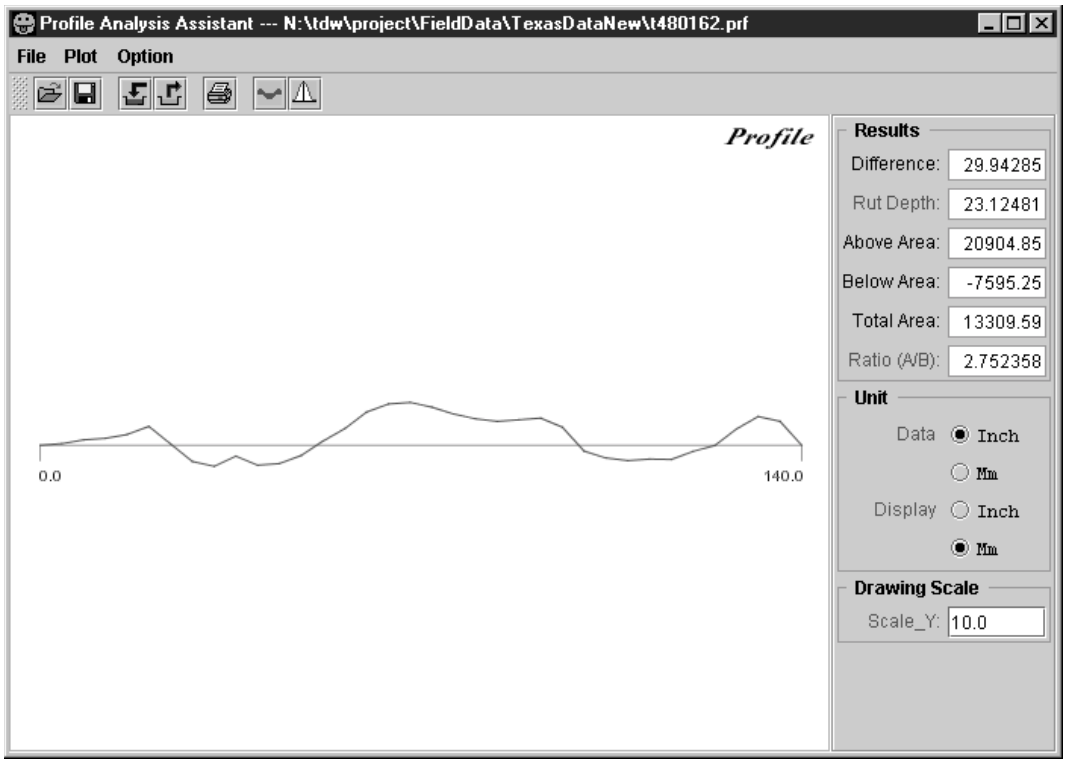

(b) surface profile and distortion parameters

Figure 6-33. Profiles of Section 480162, US 281, Texas.

Figure 6-34. The straightedge device.

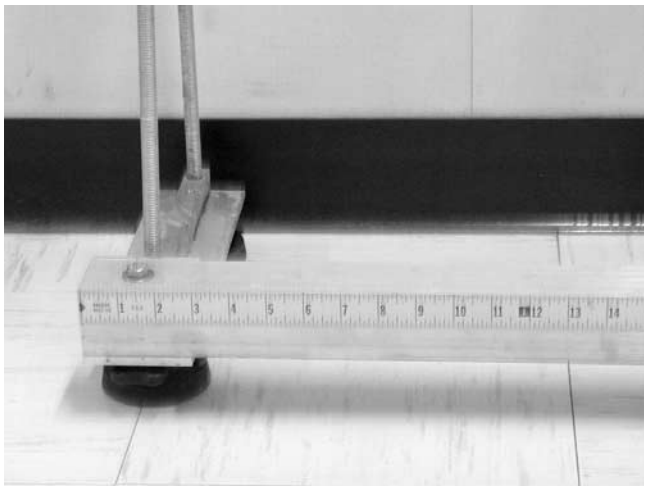

Figure 6-35. Adjustable support at the left end of the straightedge.

Figure 6-36. Adjustable support in the middle of the straightedge.

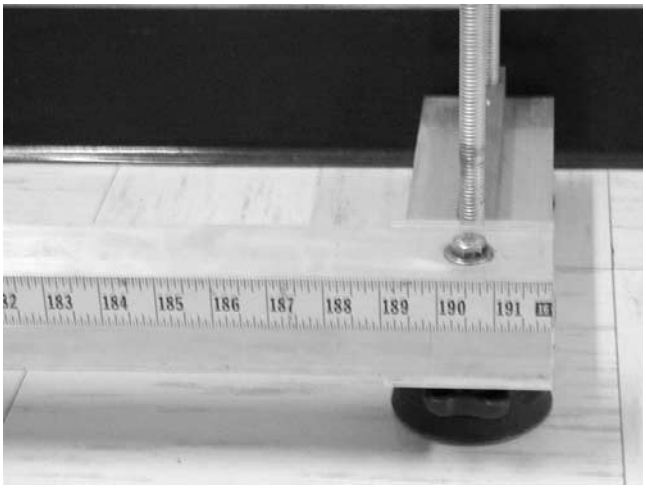

Figure 6-37. Adjustable support at the right end of the straightedge.

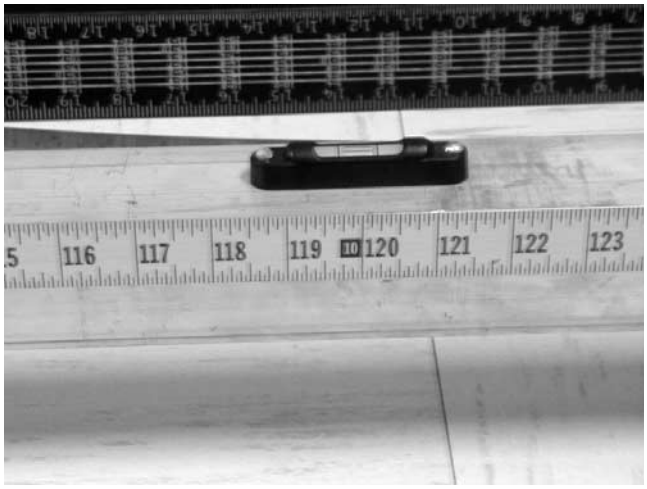

Figure 6-38. Leveling bar on top of the straightedge.

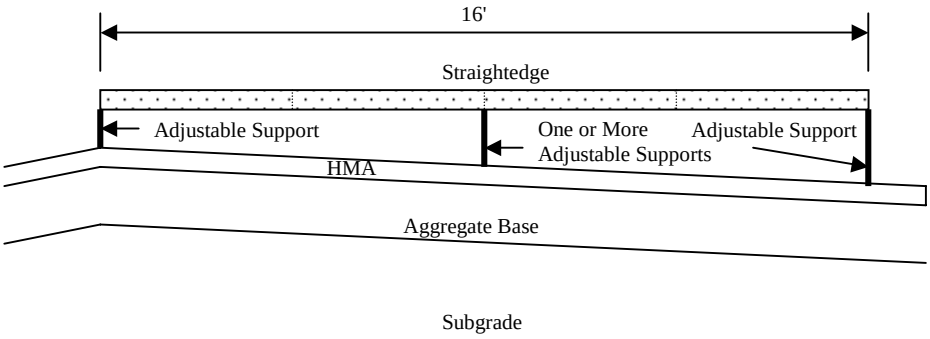

Figure 6-39. Pavement cross section showing straightedge setup.

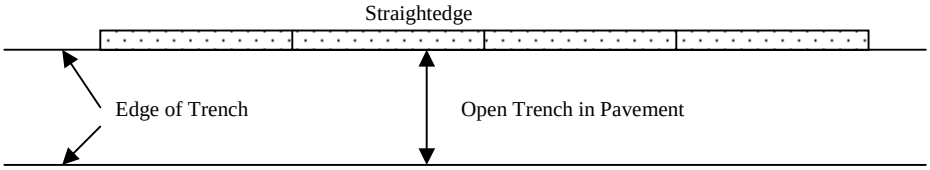

Figure 6-40. Plan view of straightedge set up along trench.

CHAPTER 7

CONCLUSIONS AND RECOMMENDATIONS

7.1 CONCLUSIONS

7.1.1 Findings

The stated goals of this study were to (1) investigate whether the relative contributions of the layers to rutting in flexible pavement could be determined from an analysis of its transverse surface profile and (2) prepare a method for estimating the relative contributions of pavement layers to total rutting. Previous research indicated that the goals were feasible. Using data from available literature, theoretical FEM analysis, and pavement trenching, these project goals were achieved. Finite element analysis proved to be an effective tool in this study. Unlike other analytical approaches, finite element analysis is able to fairly represent layer and pavement geometry, material characteristics, boundary conditions, and loading. In particular, failure strains in a layer are promulgated and captured in surface deformations. The resulting surface deformations match very well the surface deformations of pavements subjected to prototype scale truck loading.

The previous research to develop surface deformation criteria for predicting layer failure was identified, and a review of this work—as well as publications by others attempting to establish similar criteria—was beneficial to the current research. In fact, surface deformation criteria reported in the literature were used to establish the important factors and their possible levels for the finite element analysis of the current study. Using finite element analysis, a matrix of pavement sections was developed, covering a range of layer materials and thicknesses. Predicted transverse surface profiles for pavement sections represented in the matrix were analyzed, and improved surface distortion criteria were developed.

In order to provide a convenient product to the user, a computer program was developed to assist users in calculating the surface distortion parameters. The program, PAAP, was initially developed to accelerate the processes of preparing finite element input data and retrieving the results from finite element output. However, PAAP can also be used to calculate surface distortion parameters from a measured surface transverse profile. The measured profile is simply entered into PAAP, and the program generates the surface distortion criteria. These distortion criteria have been formatted for use in a spreadsheet named "failure identification table" (FIT). When the criteria are entered into FIT, the failed layer is identified and the results are plotted on a failure chart. Examples of these results are given in Chapter 5. A draft transverse surface profile measurement and analysis standard has been prepared in AASHTO format and included in this report (see appendix). The standard includes guidance on the spacing of transverse surface profile measurements, as well as steps for using the criteria to predict the location of the failed layer in the pavement structure.

In addition to developing refined surface distortion criteria, finite element analysis was used to examine factors that can affect the application of the criteria. Specifically, very thin asphalt surfaces may not protect an underlying base. In this case, the base fails and the surface distortion wrongly classifies the failure as being in the surface layer. Finite element analysis predicted this phenomenon, and field data confirmed it. The criteria developed through this project handle this condition as a special case.

Also, required transverse spacing of surface profile measurements was examined using the FEM-predicted surface profiles. By eliminating surface profile data points and recalculating surface distortion parameters, maximum allowable data point spacing was determined. To maintain criteria accuracy, maximum spacing for surface, base, and subgrade failures are 100 mm (4 in.), 175 mm (7 in.), and 300 mm (12 in.), respectively. Because the layer contributing to pavement failure is not known when the profile is measured, the maximum spacing should be 100 mm (4 in.).

The effects of pavement shoulders on surface distortion were also examined; pavements with and without paved shoulder were analyzed. A specific result of this analysis is that the distortion parameters are independent of the paved shoulder width as long as the surface profile of the lane or lane-plus-shoulder segment is 3.7 m (12 ft) wide. When the lane is narrower than 3.7 m (12 ft) but has a paved shoulder (for example, a 3.1-m [10-ft] lane), the transverse profile should extend onto the shoulder so that the total width of the profile is 3.7 m (12 ft). If the profile width is less than 3.7 m (12 ft), the results may not be reliable for base failure.

Significant information was obtained from trench data. The most important result was that the refined surface distortion criteria were confirmed. Another result was that the majority of the pavements investigated in this study exhibited rutting in

the asphalt layers (i.e., the top 75–125 mm [3–5 in.]). This result agrees with other recent studies of pavement rutting.

7.1.2 Applicability

The proposed criteria for predicting layer failure from a pavement's transverse surface profile are material independent. However, identifying a layer as failed can highlight deficiencies in materials, specifications, construction, and structural design. The criteria can be applied at the project or network level.

Application of the proposed criteria to transverse surface profiles from a specific project will identify the lowermost layer contributing to rutting. As a result, appropriate remedial action plans can be developed. For example, subgrade failure could be addressed by reconstruction (including subgrade stabilization, placement of adequate pavement structural layer thickness, or both). Alternatively, additional HMA thickness could be placed to increase the structural section and to protect the subgrade. If the failure is associated with the HMA surface layer, then the affected depth or the entire surface could be removed by grinding and replaced with an overlay (i.e., the surface could undergo a mill-and-fill operation). Alternatively, multiple overlays can be placed to build a smooth, stable surface. A combination of partial-depth grinding and overlay can also be used.

The study results also apply to pavement networks. When applied at the network level, the criteria become a powerful management tool. For example, sufficiency of materials, tests, specifications, construction, and thickness design can be evaluated on a systemwide basis. As a result, the need for corrective action would be well supported. The need for areas of research to improve the insufficient parameter would also be identified.

7.2 RECOMMENDATIONS

The research team believes that state departments of transportation and other user agencies can immediately implement the findings of this study. To this end, an implementation effort is recommended. The main tasks of such an effort would be to

1. Identify state departments of transportation willing to participate in the implementation effort;
2. Provide software, training, and assistance to these departments on how to properly use the software and apply the criteria;
3. Assist the departments in collecting data; and
4. Analyze the results of the implementation effort and update the software criteria, standard test method, or both as needed.

An additional benefit of the implementation effort would be to provide additional verification of the proposed criteria. The choice of pavement sections included in the current study for criteria verification could not be well controlled, as data for pavement layer failures depended on agency participation. A consequence is that not all pavement layer failures are represented in the database at the desired level of replication. Specifically, subgrade failure data are limited. This situation is not expected to affect the surface distortion criteria for subgrade failure. The currently available data clearly support the FEM-based criteria. New data will only strengthen confidence in the criteria for all layers.

In addition to the main goals outlined previously, an implementation study could also address the question of transverse profile longitudinal spacing. Variation in transverse surface profiles is expected. The question to be answered is, "How many transverse surface profiles should be measured, and at what spacing should they be measured, to accurately determine a failed layer?" This issue should be addressed at both the project level and the network level.

A finding of the current study is that transverse spacing of surface profile measurements is important. Without a spacing of 75–100 mm (3–4 in.), details of the surface distortion are not adequately captured. Agency protocols for field data collection of transverse surface profiles should be revised to agree with the draft standard in the appendix. This recommendation can be implemented immediately when manual measurements are used. Agencies using electronic devices that record a continuous transverse profile can use such data with the appropriate measurement spacing. Measur-ing transverse profiles manually or with an electronic device is time consuming. Application is likely to be limited to project-level evaluations. A faster method of collecting transverse surface profile data will be required for network-level evaluations.

Existing equipment that is used to obtain data on surface transverse profiles at the network level operates at highway speeds and has three to five sensors perpendicular to the direction of travel. The current study indicates that the usual sensor spacing of these devices is inadequate to correctly determine the layer in which rutting is occurring. Certainly, the spacing is not adequate for calculating surface distortion parameters. The research team recommends making an effort to refine existing technology or develop new technology capable of adequately measuring a transverse surface profile with the required precision at highway speeds.

A scanning laser is candidate technology for measuring transverse pavement surface profiles. There are at least two such laser systems currently available. One device [50] has been used at WesTrack and is currently being investigated at the U.S. Army Corps of Engineers Engineering Research and

Development Center, Vicksburg, Mississippi. Another laser system has been developed at the Diagnostic Instrumentation and Analysis Laboratory (DIAL) at Mississippi State University, Starkville, Mississippi. An effort is recommended to develop a scanning-laser–based system for measuring transverse pavement surface profiles. This type of system offers the best possibility of measuring transverse profiles with the desired accuracy at highway speeds.

Finally, one possible aspect of an implementation effort might be to develop guidelines about milling depth when rehabilitating HMA pavements. These guidelines could serve as a valuable tool when user agencies are unsure of the existing cross section of a pavement exhibiting permanent deformation. An initial effort to develop such guidelines was attempted; the additional data collected in the implementation effort could assist in perfecting this tool.

REFERENCES

1. Middleton, D. R., F. L. Roberts, and T. Chira-Chavala, "Measurements and Analysis of Truck Tire Pressures on Texas Highways," *Transportation Research Record 1070,* Transportation Research Board, National Research Council, Washington, D.C., 1986.
2. Proceedings, "A Symposium/Workshop on High Pressure Truck Tires," American Association of State Highway and Transportation Officials and Federal Highway Administration, Austin, Texas, February 1987.
3. Ford, M. C., "Development of a Rational Mix Design Method for Asphalt Bases and Characteristics of Arkansas Asphalt Mixtures," *FHWA-AR-85-004,* Federal Highway Administration, U.S. Department of Transportation, Washington, D.C., July 1985.
4. Kandhal, P., S. A. Cross, and E. R. Brown, "Evaluation of Bituminous Pavements for High Pressure Truck Tires," *FHWA-PA-90-008-87-01,* Federal Highway Administration, U.S. Department of Transportation, Washington, D.C., December 1990.
5. Brown, E. R., and S. A. Cross, "A National Study of Rutting in Hot Mix Asphalt (HMA) Pavements," *NCAT Report 92-5,* National Center for Asphalt Technology, Auburn, Alabama, 1992.
6. Monismith, C. L., R. G. Hicks, F. M. Finn, J. Sousa, J. Harvey, S. Weissman, J. Deacon, J. Coplantz, and G. Paulsen, "Permanent Deformation Response of Asphalt Aggregate Mixes," *SHRP-A-415,* Strategic Highway Research Program, Transportation Research Board, National Research Council, Washington, D.C., 1994.
7. Kennedy, T. W., G. A. Huber, E. G. Harrigan, R. J. Cominsky, C. S. Hughes, H. Von Quintas, and J. S. Moulthrop, "Superior Performing Asphalt Pavements (Superpave): The Product of the SHRP Asphalt Research Program," *SHRP-A-410,* Strategic Highway Research Program, Transportation Research Board, National Research Council, Washington, D.C., 1994.
8. Harrigan, E. G., R. B. Leahy, and J. S. Youcheff, "The Superpave Mix Design System Manual of Specifications, Test Methods, and Specifications," *SHRP-A-379,* Strategic Highway Research Program, Transportation Research Board, National Research Council, Washington, D.C., 1994.
9. Witczak, M. W., H. Von Quintas, and C. W. Schwartz, "Superpave Support and Performance Models Management: Evaluation of the SHRP Performance Models System," Proceedings of the Eighth International Conference on Asphalt Pavements, Vol. 3, August 1997.
10. Yoder, E. J., and M. W. Witczak, *Principles of Pavement Design,* John Wiley and Sons, Inc., New York, New York, 1975.
11. Simpson, A., "Characterization of Transverse Profile," *Transportation Research Record 1655,* Transportation Research Board, National Research Council, Washington, D.C., 1999.
12. Epps, J. A., C. L. Monismith, S. B. Seeds, S. H. Alavi, S. C. Ashmore, R. B. Leahy, and T. M. Mitchell, "WesTrack Performance—Interim Findings," *Journal of the Association of Asphalt Paving Technologists,* Vol. 67, Association of Asphalt Paving Technologists, St. Paul, Minnesota, 1998.
13. Gramling, W. L., J. E. Hunt, and G. Suzuki, "Rational Approach to Cross-Profile and Rut Depth Analysis," *Transportation Research Record 1311,* Transportation Research Board, National Research Council, Washington, D.C., 1991.
14. Oteng-Seifah, S., and P. G. Manke, "Study of Rutting in Flexible Highway Pavements in Oklahoma," *Transportation Research Record 602,* Transportation Research Board, National Research Council, Washington, D.C., 1976.
15. Mahboub, K., A. Simpson, P. Oduroh, and J. Fleckenstein, "Field Performance of Large-Stone Hot Mix Asphalt on a Kentucky Coal Haul Road," *Transportation Research Record 1337,* Transportation Research Board, National Research Council, Washington, D.C., 1992.
16. Brown, E. R., and S. A. Cross, "A Study of In Place Rutting of Asphalt Pavements," *Journal of the Association of Asphalt Paving Technologists,* Vol. 58, Association of Asphalt Paving Technologists, St. Paul, Minnesota, 1989.
17. Brown, E. R., and S. A. Cross, "A Study of Rutting in Hot Mix Asphalt (HMA) Pavements," *Journal of the Association of Asphalt Paving Technologists,* Vol. 61, Association of Asphalt Paving Technologists, St. Paul, Minnesota, 1992.
18. Dawley, C. B., B. L. Hogewiede, and K. O. Anderson, "Mitigation of Instability Rutting of Asphalt Concrete Pavements in Lethbridge, Alberta, Canada," *Journal of the Association of Asphalt Paving Technologists,* Vol. 59, Association of Asphalt Paving Technologists, St. Paul, Minnesota, 1990.
19. Lenngren, C. A., "Some Approaches in Treating Automatically Collected Data on Rutting," *Transportation Research Record 1196,* Transportation Research Board, National Research Council, Washington, D.C., 1988.
20. Simpson, A. L., J. F. Daleiden, and W. O. Hadley, "Rutting Analysis From a Different Perspective," *Transportation Research Record 1473,* Transportation Research Board, National Research Council, Washington, D.C., 1995.
21. Brown, S. F., and J. M. Gibb, "Validation Experiments for Permanent Deformation Testing of Bituminous Mixtures," *Journal of the Association of Asphalt Paving Technologists,* Vol. 65, Association of Asphalt Paving Technologists, St. Paul, Minnesota, 1996.
22. Odermatt, N., V. Janoo, and R. Magnusson, "Analysis of Permanent Deformation in Subgrade Material Using a Heavy Vehicle Simulator," preprint of Proceedings of the International Conference on Accelerated Pavement Testing, Reno, Nevada, October 1999.
23. Nokes, W. A., J. T. Harvey, L. du Pleisses, F. Long, and P. J. Stolarski, "CALTRANS Accelerated Pavement Testing (CAL/APT) Program—Test Results: 1993–1996," Proceedings of the Eighth International Conference on Asphalt Pavements, Vol. 2, Seattle, Washington, August 1997.
24. Harvey, J., "Initial CAL/APT Program: Site Information, Test Pavements Construction, Pavement Materials Characterization, Initial CAL/HVS Test Results, and Performance Estimates," report for the California Department of Transportation, Institute of Transportation Studies, University of California, Berkeley, 1996.

25. Prozzi, J., J. T. Harvey, J. Deacon, I. Guada, and D. Hung, "Analysis of Observed and Predicted Performance for CAL/APT Flexible Pavement Sections," *77th Annual Meeting Preprint CD-ROM*, Transportation Research Board, National Research Council, Washington, D.C., 1998.
26. Chen, D. H., K. Fults, and M. Murphy, "Primary Results for the First Texas Mobile Load Simulator Test Pad," *Transportation Research Record 1570*, Transportation Research Board, National Research Council, Washington, D.C., 1997.
27. Chen, D. H., and F. Hugo, "Full-Scale Accelerated Pavement Testing of Texas Mobile Load Simulator," *Journal of Transportation Engineering*, Vol. 24, No. 5, September/October, American Society of Civil Engineers, 1998.
28. Hugo, F., A. de Fortier Smit, and P. Warren, "Report on APT Data Survey," *Transportation Research Circular E-C004*, Transportation Research Board, National Research Council, Washington, D.C., February 1999.
29. Chen, D.-H., J. Bilyeu, D. Walker, and M. Murphy, "Study of Rut-Depth Measurements," *80th Annual Meeting Preprint CD-ROM*, Transportation Research Board, National Research Council, Washington, D.C., 2001.
30. Bonaquist, R. J., and W. S. Mogawer, "Analysis of Pavement Rutting Data from FHWA Pavement Testing Facility Superpave Validation Study," *Transportation Research Record 1590*, Transportation Research Board, National Research Council, Washington, D.C., 1997.
31. Bonaquist, R., J. Sherwood, and K. Stuart, "Accelerated Pavement Testing at the Federal Highway Administration Pavement Testing Facility," *Journal of the Association of Asphalt Paving Technologists*, Vol. 67, Association of Asphalt Paving Technologists, St. Paul, Minnesota, 1998.
32. Epps, J. A., C. L. Monismith, S. B. Seeds, S. H. Alavi, S. C. Ashmore, R. B. Leahy, and T. M. Mitchell, "WesTrack Full-Scale Test Track: Interim Findings," Proceedings of the Eighth International Conference on Asphalt Pavements, Vol. 3, August 1997.
33. D'Angelo, J. A., "What's Happening at WesTrack," *FOCUS*, Federal Highway Administration, U.S. Department of Transportation, Washington, D.C., September 1996.
34. Hand, A. J., J. A. Epps, and P. E. Sebaaly, "Precision of ASTM D5821: Standard Test Method for Determining the Percentage of Fractured Particles in Coarse Aggregate," *ASTM Journal of Testing and Evaluation*, Vol. 28, No. 2, March 2000, pp. 67–76.
35. Sousa, J. B., and S. L. Weissman, "Modeling Permanent Deformation of Asphalt-Aggregate Mixes," *Journal of the Association of Asphalt Paving Technologists*, Vol. 63, Association of Asphalt Paving Technologists, St. Paul, Minnesota, 1994, pp. 224–256.
36. Sousa, J. B., "Asphalt-Aggregate Mix Design Using the Repetitive Simple Shear Test (Constant Height)," *Journal of the Association of Asphalt Paving Technologists*, Vol. 63, Association of Asphalt Paving Technologists, St. Paul, Minnesota, 1994, pp. 298–345.
37. Sousa, J. B., S. L. Weissman, J. L. Sackman, and C. L. Monismith, "Nonlinear Elastic Viscous with Damage Model to Predict Permanent Deformation of Asphalt Concrete Mixes," *Transportation Research Record 1384*, Transportation Research Board, National Research Council, Washington, D.C., 1993.
38. Lytton, R. L., J. Uzan, E. G. Fernando, R. Roque, D. Hiltunen, and S. M. Stoffels, "Development and Validation of Performance Prediction Models and Specifications for Asphalt Binders and Paving Mixes," *SHRP-A-357*, Strategic Highway Research Program, Transportation Research Board, National Research Council, Washington, D.C., 1993.
39. Hopman, P. C., R. N. Nilsson, and A. C. Pronk, "Theory, Validation and Application of the Visco-Elastic Multilayer Program VEROAD," Proceedings of the Eighth International Conference on Asphalt Pavements, Vol. 2, Seattle, Washington, August 1997.
40. Nilsson, R. N., and P. C. Hopman, "Viscoelastic Analysis of Full-Scale Pavements: Validation of VEROAD," *Transportation Research Record 1539*, Transportation Research Board, National Research Council, Washington, D.C., 1997.
41. Hopman, P. C., "VEROAD: A Viscoelastic Multilayer Computer Program," *Transportation Research Record 1539*, Transportation Research Board, National Research Council, Washington, D.C., 1997.
42. Yandell, W. O., and G. Behzadi, "Performance Prediction of Accelerated Loading Facility (ALF) Trials Using Elastic, Visco-Elastic, and Elasto-Plastic Analysis," Proceedings of the Eighth International Conference on Asphalt Pavements, Vol. 2, Seattle, Washington, August 1997.
43. Yandell, W. O., "Measurement and Prediction of Forward Movement and Rutting in Pavements Under Repetitive Wheel Loads," *Transportation Research Record 888*, Transportation Research Board, National Research Council, Washington, D.C., 1983.
44. Huang, H., and T. D. White, "Modeling and Analysis of Accelerated Pavement Tests," *77th Annual Meeting Preprint CD-ROM*, Transportation Research Board, National Research Council, Washington, D.C., 1998.
45. Zaghloul, S., and T. D. White, "Guidelines for Permitting Overloads PART I: Effect of Overloaded Vehicles on the Indiana Highway Network," Joint Highway Research Project, FHWA/INDOT/JHRP-93/5, Purdue University, 1994.
46. White, T. D., S. M. Zaghloul, G. L. Anderson, and D. M. Smith, "Pavement Analysis for Moving Aircraft Loads," *ASCE Journal of Transportation Engineering*, Vol. 126, No. 6., November/December 1997, pp. 436–446.
47. Haddock, J., C. Pan, A. Feng, K. Galal, and T. D. White, "National Pooled Fund Study No. 176: Validation of SHRP Asphalt Mixture Specifications Using Accelerated Testing," interim report, Indiana Department of Transportation, September 1998.
48. White, T. D., J. M. Albers, and J. E. Haddock, "Limiting Design Parameters for a Pavement Accelerated Testing System," American Society of Civil Engineers, *Journal of Transportation Engineering*, Vol. 118, No. 6, 1992, pp. 787–804.
49. Huang, H. M., "Analysis of Accelerated Pavement Tests and Finite Element Modeling of Rutting Phenomenon," Ph.D. thesis, Purdue University, West Lafayette, Indiana, August 1995.
50. Galal, K. A., and T. D. White, "INDOT-APT Facility Experience," Preprint of Proceedings of the International Conference on Accelerated Pavement Testing, Reno, Nevada, October 1999.
51. White, T. D., J. Hua, and K. A. Galal, "Analysis of Accelerated Pavement Tests," Preprint of Proceedings of the International Conference on Accelerated Pavement Testing, Reno, Nevada, October 1999.
52. Hand, A. J., K. A. Galal, D. R. Ward, and C. Fang, "Cost-Effectiveness of Joint and Crack Sealing: Synthesis of Prac-

tice," *ASCE Journal of Transportation Engineering*, Vol. 126, No. 6, November/ December 2000, pp. 521–529.

53. Hua, J., "Finite Element Modeling and Analysis of Accelerated Pavement Testing Devices and Phenomenon," thesis submitted to Purdue University, August 2000.
54. Chadbourn, B. A., D. E. Newcomb, and D. H. Timm, "Measured and Theoretical Comparisons of Traffic Loads and Pavement Response Distributions," Proceedings of the Eighth International Conference on Asphalt Pavements, Vol. 1, Seattle, Washington, August 1997.
55. Buiter, R., W. M. H. Cortenraad, A. C. van Eck, and H. van Rij, "Effects of Transverse Distribution of Heavy Vehicles on Thickness Design of Full-Depth Asphalt Pavements," *Transportation Research Record 1227*, Transportation Research Board, Washington, D.C., 1989.
56. De Beer, M., C. Fisher, and F. J. Jooste, "Determination of Pneumatic Tire/Pavement Interface Contact Stresses Under Moving Loads and Some Effects on Pavements with Thin Asphalt Layers," Proceedings of the Eighth International Conference on Asphalt Pavements, Vol. 1, Seattle, Washington, August 1997, pp. 129–139.
57. Himeno, K., and T. Ikeda, "Distribution of Tire Contact Pressure of Vehicles and Its Influence on Pavement Distress," Proceedings of the Eighth International Conference on Asphalt Pavements, Vol. 1, Seattle, Washington, August 1997, pp. 179–227.
58. Taragin, A., "Effects of Roadway Width on Vehicle Operation," *Public Roads*, Vol. 24, No. 6, pp. 143–160, December 1945.
59. Taragin, A., "Driver Behavior Related to Types and Widths of Shoulders on Two-Lane Highways," *Public Roads*, Vol. 29, No. 9, August 1957, pp. 197–205.
60. Taragin, A., "Lateral Placements of Trucks on Two-Lane Highways and Four-Lane Divided Highways," *Public Roads*, Vol. 30, No. 3, August 1958, pp. 71–75.
61. Kasahara, A., "Wheel Path Distribution of Vehicles on Highway," Proceedings of the International Symposium on Bearing Capacity of Roads and Airfields, Vol. 1, Trondheim, Norway, June 1982, pp. 413–420.
62. Miller, I., J. E. Freud, and R. A. Johnson, *Probability and Statistics for Engineers*, Fourth Edition, Prentice Hall, Englewood Cliffs, New Jersey, 1990.
63. ERES Consultant and Fugro-BRE, "Determination of Traffic Information and Data for Pavement Structural Design and Evaluation," interim report for NCHRP Project 1-37A, Transportation Research Board, National Research Council, Washington, D.C., December 1999.
64. De Beer, M., J. Groenendijk, and C. Fisher, "Three-Dimensional Contact Stresses under the LINTRACK Wide Base Single Tyres, Measured with the Vehicle-Road Surface Pressure Transducer Array (VRSPTA) System in South Africa," Confidential Contract Report CR-96/056, November 1996.
65. Parker Jr., F., and E. R. Brown, "A Study of Rutting of Alabama Asphalt Pavements," Alabama Department of Transportation, final report for Project 2019-09, Bureau of Research and Development, Montgomery, Alabama, November 1993.
66. Isackson, C., D. Boerner, and S. Dai, "Minnesota Road Research Forensic Investigation," draft final report, Office of Research Services, Minnesota Department of Transportation, St. Paul, Minnesota, July 1999.
67. Sargand, S. M., B. A. Young, I. S. Khoury, D. L. Wasniak, and B. M. Goldsberry, "Final Report on Forensic Study for Section 390101 of Ohio SHRP US 23 Test Pavement," Ohio Department of Transportation and Federal Highway Administration, Columbus, Ohio, February 1998.
68. Chen, D.-H., J. Bilyeu, M. Murphy, and D. Walker, "Comparison of Rut-Depth Measurements," draft of a paper submitted to the Transportation Research Board for consideration for presentation and publication at the 80th Annual Meeting of the Transportation Research Board, Washington, D.C., by the Texas Department of Transportation, Austin, Texas, July 2000.
69. Chen, D.-H., T. Scullion, J. Bilyeu, D.-F. Lin, and F. Zhou, "Forensic Evaluation of the Premature Failures of the SPS-1," draft paper Texas Department of Transportation, Austin, Texas, January 2001. Copies can be obtained by contacting dchen@dot. state.tx.us.

GLOSSARY OF ACRONYMS AND ABBREVIATIONS

AAPT: Association of Asphalt Paving Technologists
AASHO: American Association of State Highway Officials
AASHTO: American Association of State Highway and Transportation Officials
ALDOT: Alabama Department of Transportation
ALF: Accelerated Loading Facilities (FHWA)
APT: accelerated pavement testing
ASCE: American Society of Civil Engineers
ASTM: American Society for Testing and Materials
ATPB: asphalt-treated permeable base
AVCS: automated vehicle control systems
BB: black base
CAL/APT: California Department of Transportation Accelerated Pavement Testing
Caltrans: California Department of Transportation
CRREL: Cold Regions Research and Engineering Laboratory (U.S. Army)
CSAB: crushed stone aggregate base
CSIR: Council of Scientific and Industrial Research
DIAL: Diagnostic Instrumentation and Analysis Laboratory (Mississippi State University)
ESAL: equivalent single axle load
FEM: finite element modeling
FHWA: Federal Highway Administration (U.S.DOT)
FIT: Failure Identification Table
FM: Farm to Market
FWD: Falling Weight Deflectometer
GPS: General Pavement Studies
HMA: hot mix asphalt
HMSA: hot mix sand asphalt
HVS: Heavy Vehicle Simulator
INDOT: Indiana Department of Transportation
JVM: Java Virtual Machine
LRA: lime rock asphalt
LTB: lime-treated base
LTGB: lime-treated gravel base
LTPP: long-term pavement performance
LTS: lime-treated soil
MDOT: Mississippi Department of Transportation
MnDOT: Minnesota Department of Transportation
MnROAD: Minnesota Road Research Project (MnDOT)
NCAT: National Center for Asphalt Technology
NCDOT: North Carolina Department of Transportation
NCHRP: National Cooperative Highway Research Program
NDOT: Nevada Department of Transportation
NIMS: National Information Management System
NTIS: National Technical Information Service
ODOT: Ohio Department of Transportation
PAAP: Profile Analysis Assistant Program
PASCO: Parallel Symbolic Computation
PFS 176: Pooled Fund Study 176
PRS: performance-related specifications
PTF: Pavement Test Facility (Nottingham)
PTI: Pennsylvania Transportation Institute
SABC: stabilized aggregate base course
SBR: styrene-butadiene rubber
SCB: soil-cement base
SH: State Highway
SHRP: Strategic Highway Research Program
SR: state route
TFHRC: Turner Fairbanks Highway Research Center (FHWA)
TRB: Transportation Research Board
TRIS: Transportation Research Information Services
TxDOT: Texas Department of Transportation
TxMLS: Texas Mobile Load Simulator
USACE: U.S. Army Corps of Engineers
WIM: weigh in motion

APPENDIX

RECOMMENDED METHOD FOR DETERMINING THE FAILED LAYER OF A FLEXIBLE PAVEMENT

1 SCOPE

This method covers the procedure for determining which layer in a flexible pavement has failed because of permanent deformation by measuring and evaluating the transverse surface profile of the failed pavement. The permanent deformation can result from densification, shear failure, or shear flow.

The method is based on analysis of transverse surface profiles of 3.7-m (12-ft) pavement lanes. Surface profile measurements should not exceed 100 mm (4 in.). For 3.1-m (10-ft) pavement lanes, the surface profile features may not be fully captured. In this case, the failed layer may not be reliably predicted.

2 SAFETY

The test vehicles, as well as all attachment to them, shall comply with all applicable state and federal laws.

Extreme caution, appropriate traffic controls, and personnel safety measures shall be taken and/or used to ensure maximum safety of operating personnel and other traffic.

This method does not purport to address all safety concerns. All necessary precautions shall be taken beyond those imposed by laws and regulations.

3 DEFINITIONS

failed layer—lowest layer contributing to the pavement's permanent surface deformation.

transverse surface profile—surface profile measured on a 3.7-m (12-ft) wide pavement lane perpendicular to the direction of traffic.

reference line—straight line connecting the two end points of the transverse surface profile.

maximum rut depth—maximum rut depth determined from the transverse surface profile using the wire method. This depth is measured perpendicular to the reference line (see Figure A-1).

positive area—sum of the areas above the transverse surface profile reference line (see Figure A-2).

negative area—sum of the areas below the transverse surface profile reference line (see Figure A-2).

total area—sum of positive and negative areas.

ratio of area—absolute value of the ratio of positive area to negative area.

distortion parameters—maximum rut depth, total area, and ratio of area.

4 APPARATUS

A reference beam is needed to measure the transverse surface profile. The minimum beam width shall be equal to or greater than 3.7 m (12 ft). The beam shall incorporate adequate support(s) and/or rigidity such that no deviation of more than 1 mm (0.04 in.) occurs at any point along its length (minimum length of 3.7 m [12 ft]) from the true horizontal due to deflection. This may be verified with a taught string line and a rule after the apparatus is set up. The device must also provide stability to resist small dynamic forces, such as wind and small bumps by the operator.

A 1.2-m (4-ft) or longer carpenter's level or a surveyor's level capable of being used to ensure that the straightedge provides a level horizontal reference when correctly set up is needed.

An adequately rigid rule or caliper of adequate length (greater than the maximum distance from the straightedge to pavement surface) is needed with a maximum increment of 1 mm (0.04 in.) for measurement.

A 5-m (16.4-ft) builder's string line is needed.

Miscellaneous hand tools are needed to ensure that the pavement surface is swept clean and free of debris prior to profile measurement.

Miscellaneous data-recording things are needed—for example, data collection forms, note pads, paper clips, and pens/pencils.

An alternative device, such as a pavement surface profiler (PSP), may be used. The PSP is a beam with attachments to trace or electronically record a continuous transverse surface profile. Maximum spacing of data for analysis of the surface profile shall be 100 mm (4 in.).

5 PROCEDURE

The procedure for determining the failed layer of a flexible pavement is as follows:

1. Establish safe working conditions for both operators and motoring public in accordance with agency policies.
2. Clean the area of pavement to be measured free of debris by sweeping.
3. Position the apparatus perpendicular to the direction of traffic. Take care to ensure that both edges of the lane can be included in the surface profile.

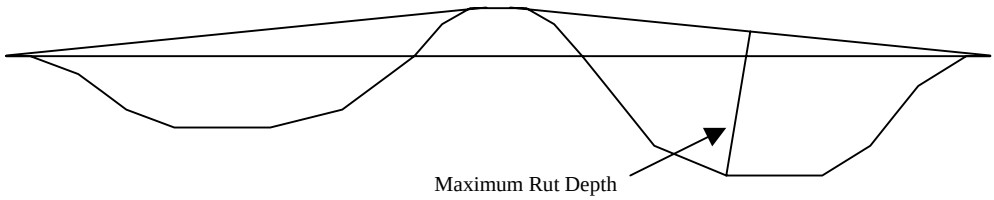

Figure A-1. Definition of maximum rut depth.

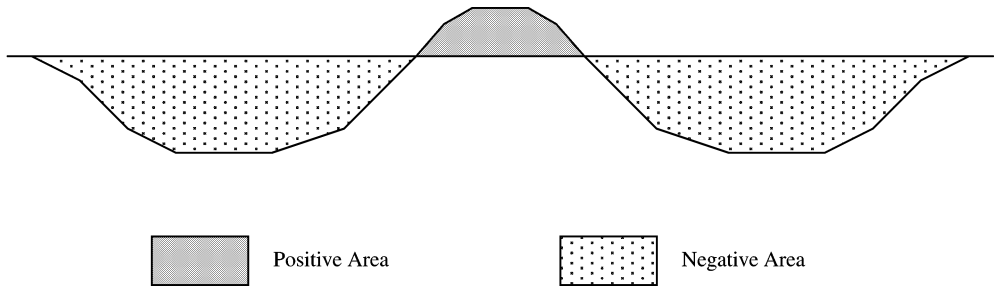

Figure A-2. Definition of positive and negative areas.

4. Adequately support the apparatus such that wind, the weight of measurement devices, small bumps by the operator, and any other potential source of reasonably small dynamic force will not move the device and force the operation to be halted and restarted. Sand and/or lead bags have been found to be a good source of leg stabilizer.
5. Adjust the apparatus supports so that the apparatus is horizontally level (see Figure A-3). Verify that no deviations greater than 1 mm (0.04 in.) from the horizontal level exist using a taught string line and a rule or caliper.
6. Starting from the inner edge of the lane, measure the vertical distance from the reference beam to the pavement surface. Continue measurements at a maximum increment of 100 mm (4 in.) for the full width of the lane, including the outside of the lane.
7. Plot the data by hand on coordinate paper or electronically using a spreadsheet or other utility program.
8. Connect the first and last data points with a straight line. Calculate the maximum rut depth, positive and negative areas, total area, and ratio of area, as described in Section 6.

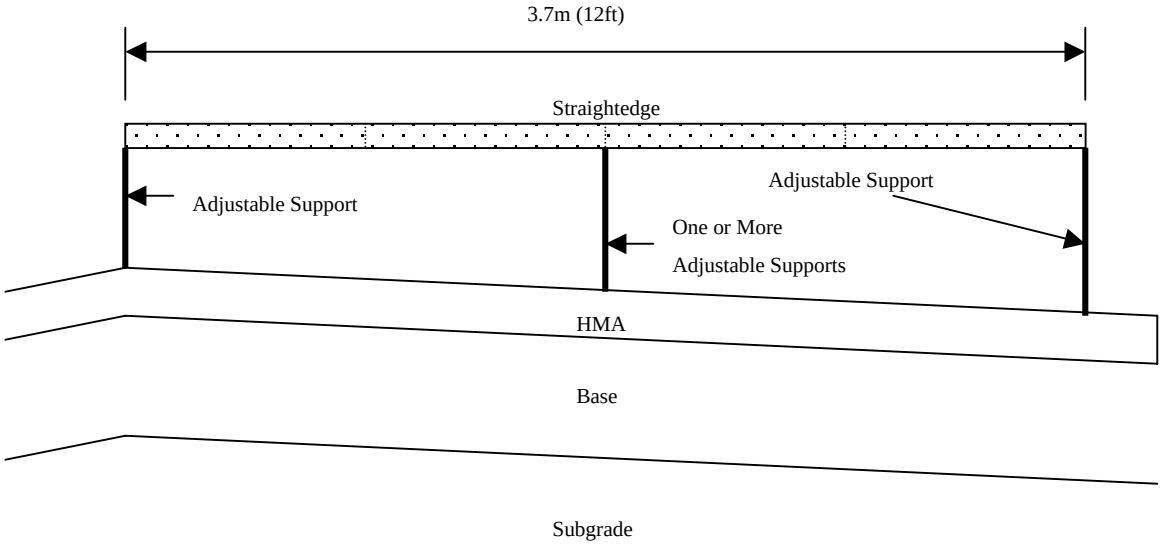

Figure A-3. Pavement cross section showing straightedge setup.

9. Determine which layer caused failure by referencing the failure criteria given in Section 6.

6 CALCULATIONS

6.1 Calculating the Distortion Parameters Using PAAP

Use any text editor to input the measured data in the following format:

N
X_1, Y_1
X_2, Y_2
…
X_N, Y_N

where

N = total number of measured data points (each data point is an [X, Y] pair);
X_i = the horizontal distance from the ith point to the centerline, $i = 1, 2, \ldots N$; and
Y_i = elevation of the ith data point, $i = 1, 2, \ldots N$. If the measurement is the distance from the device (e.g., a straightedge) to the data point, the elevation is the negative value of this distance.

Save the text file with extension name ".prf". Run PAAP and open this data file. The profile will be plotted on the left side, and the *distortion parameters* will be reported on the right side. The parameters are *rut depth* (D), *above area* (A_p), *below area* (A_n), *total area* (A), and *ratio* (R). The first parameter is the maximum rut depth from the profile. *Above area* and *below area* are the positive and negative areas; *ratio* is the ratio of area. See Section 3 for these definitions. *Total area* and *ratio* are calculated as follows:

$$A = A_p + A_n \tag{A-1}$$

$$R = |A_p / A_n| \tag{A-2}$$

6.2 Determining the Failure Mode Using the Failure Identification Table (FIT)

Input the *maximum rut depth* (D), *total area* (A), and *ratio of area* (R) from Section 6.1 in the corresponding columns in the same row in FIT. The three columns are on the left side of a shaded strip in the table. The failure mode will be shown in one of the three columns to the right of the shaded strip on the same row by a mark "x." The three columns correspond to HMA failure, base failure, and subgrade failure, respectively. The data point is also shown in the failure chart.

6.3 Determine the Failure Mode Manually

Calculate critical coefficients.

$$C_1 = (-858.21)D + 667.58 \tag{A-3}$$

$$C_2 = (-1,509.0)D - 287.78 \tag{A-4}$$

$$C_3 = (-2,120.1)D - 407.95 \tag{A-5}$$

where

C_1 = theoretical average total area for HMA failure, mm^2;
C_2 = theoretical average total area for base/subbase failure, mm^2;
C_3 = theoretical average total area for subgrade failure, mm^2; and
D = maximum rut depth, mm.

The theoretical average total areas are points on the trend lines corresponding to the rut depth D in the failure chart.

Failure has occurred in the HMA layer if both the following conditions are satisfied:

$$R > 0.05 \tag{A-6}$$

$$A > (C_1 + C_2)/2 \tag{A-7}$$

If both of the above conditions are not satisfied, but strong curvature reversal is found between the two ruts, the HMA layer has failed.

If the conditions of Equations A-6 and A-7 and the conditions of the previous paragraph indicate that failure did not occur in the HMA layer, the following comparison is made:

$$A > (C_2 + C_3)/2 \tag{A-8}$$

If this condition is satisfied, failure occurred in the base/subbase layer.

Subgrade failure has occurred if no failure can be determined from the previous comparisons.

All the above comparisons for *total area* use real numbers rather than absolute values. For example, if

$$A = -15,000\text{mm}^2 \tag{A-9}$$

and

$$(C_1 + C_2)/2 = -16,000\text{mm}^2, \tag{A-10}$$

then the following condition is satisfied:

$$T > (C_1 + C_2)/2 \tag{A-11}$$

For pavement structures in which the thickness of the HMA layer is less than 75 mm (3 in.), if the above procedure indicates that the HMA layer has failed, the actual failure is in the base layer. The HMA layer may or may not have made a minor contribution to the failure.

7 EXAMPLES

7.1 Introduction

Two examples are presented to illustrate the calculation procedures given in Section 6. Section 7.2 illustrates an example of HMA failure, while Section 7.3 gives an example of base failure.

7.2 HMA Failure Example

Assume the surface profile was measured and plotted, as shown in Figure A-4. The transverse profile measurements were taken at 100-mm (4-in.) intervals. The data are shown in the table at the right of the graph (see Figure A-4). Figure A-5 gives the distortion parameters and the plotted profile generated by PAAP. The cross slope has been removed by PAAP. The *maximum rut depth* (D), *positive area* (A_p), and *negative area* (A_n) were determined to be 23 mm (0.9 in.), 20,904 mm^2 (32 in.^{2}), and –7,595 mm^2 (12 in.^{2}), respectively (the numbers have been rounded).

The *total area* (A) and *ratio of area* (R) are then calculated using Equations A-1 and A-2, respectively.

$$A = A_P + A_N = 20,904 + (-7,595) = 13.309\text{mm}^2 \quad \text{(A-12)}$$

$$R = |A_P/A_N| = |20,904/(-7,595)| = 2.75 \quad \text{(A-13)}$$

Equations A-3, A-4, and A-5 are used to calculate the three critical coefficients C_1, C_2, and C_3, respectively.

$$C_1 = (-858.21)D + 667.58 = (-858.21) \times 23.1 + 667.58 = -19,157\text{mm}^2 \quad \text{(A-14)}$$

$$C_2 = (-1,509.0)D - 287.78 = (-1.509.0) \times 23.1 - 287.78 = -35,146\text{mm}^2 \quad \text{(A-15)}$$

$$C_3 = (-2,120.1)D - 407.95 = (-2,120.1) \times 23.1 - 407.95 = -49,382\text{mm}^2 \quad \text{(A-16)}$$

Conditions in Equations A-6 and A-7 are checked and are found to be satisfied.

$$R = 2.75 \text{ (which is greater than 0.05)} \quad \text{(A-17)}$$

$$A = 13,309\text{mm}^2 \text{ (which is greater than } [C_1 + C_2]/2\text{, or } [-19,157 - 35,146]/2, \text{ or } -27,152\text{mm}^2\text{)} \quad \text{(A-18)}$$

Therefore, the failure occurred in the HMA layer. Note from the profile that curvature reversal does appear to be present. Thus, this condition is also satisfied.

7.3 Base Failure Example

Assume the surface profile was measured and plotted, as shown in Figure A-6. The transverse profile measurements were taken at an interval of 300 mm (12 in.). The data are shown in the table at the right of the graph (see Figure A-6). Figure A-7 gives the distortion parameters and the plotted profile generated by PAAP. The cross slope has been removed by PAAP. The *maximum rut depth* (D), *positive area* (A_p), and *negative area* (A_n) were determined from the profile to be 13 mm (0.5 in.), 28 mm^2 (0.04 in.^{2}), and –20,686 mm^2 (32 in.^{2}), respectively (numbers have been rounded).

The *total area* (A) and *ratio of area* (R) are calculated using Equations A-1 and A-2, respectively.

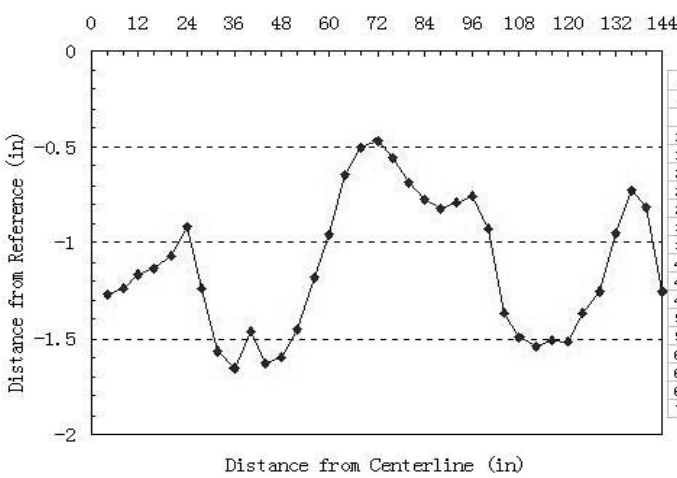

x	y	x	y
4	−1.27	76	−0.56
8	−1.24	80	−0.69
12	−1.17	84	−0.77
16	−1.14	88	−0.82
20	−1.07	92	−0.79
24	−0.92	96	−0.76
28	−1.24	100	−0.92
32	−1.57	104	−1.37
36	−1.65	108	−1.49
40	−1.47	112	−1.54
44	−1.63	116	−1.51
48	−1.6	120	−1.52
52	−1.45	124	−1.37
56	−1.19	128	−1.26
60	−0.96	132	−0.95
64	−0.65	136	−0.73
68	−0.5	140	−0.81
72	−0.47	144	−1.25

Figure A-4. Measured pavement surface profile with HMA failure.

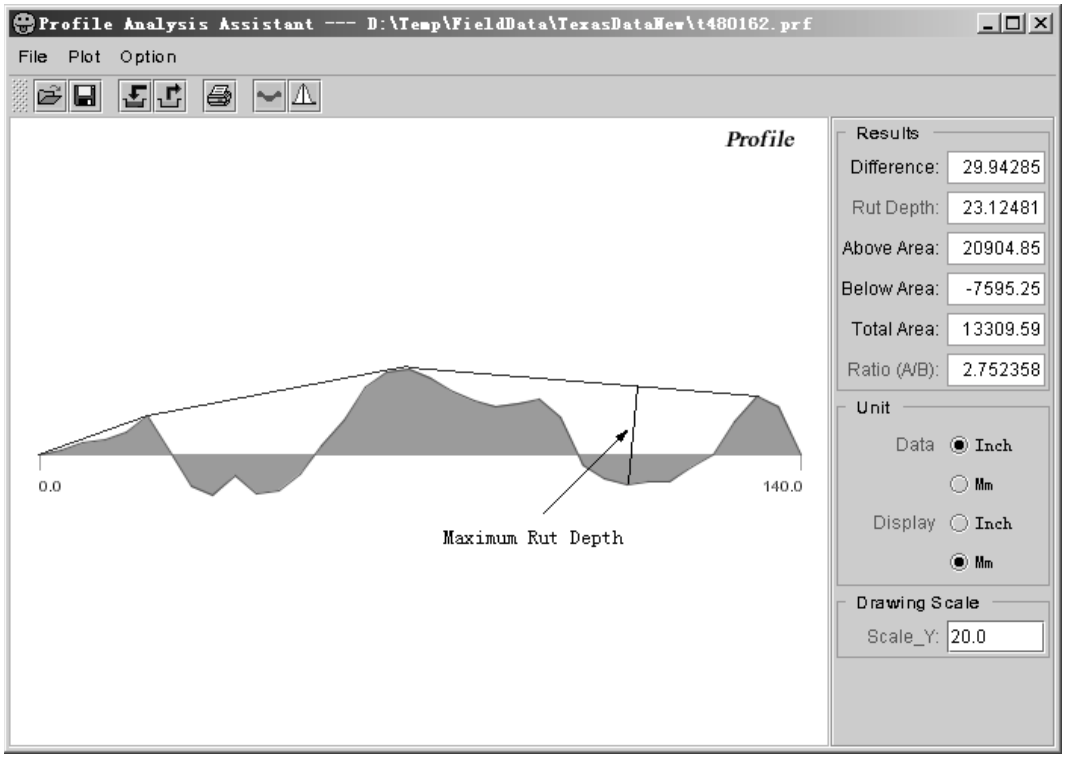

Figure A-5. Surface profile and distortion parameters for HMA failure.

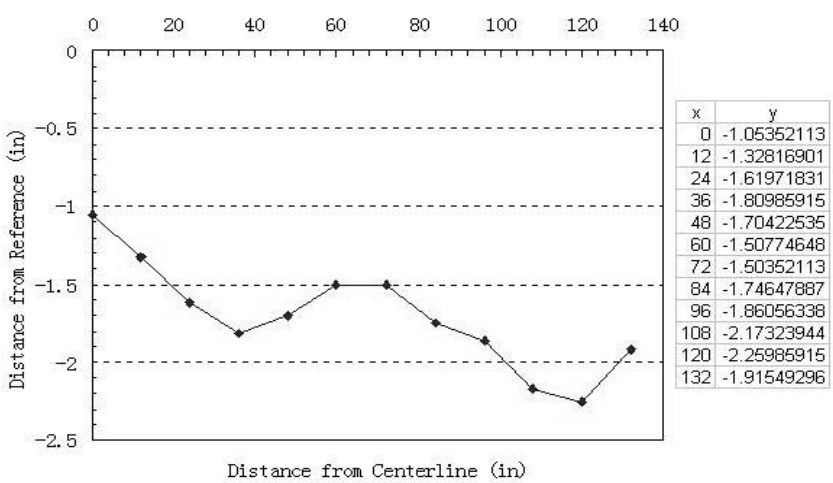

x	y
0	-1.05352113
12	-1.32816901
24	-1.61971831
36	-1.80985915
48	-1.70422535
60	-1.50774648
72	-1.50352113
84	-1.74647887
96	-1.86056338
108	-2.17323944
120	-2.25985915
132	-1.91549296

Figure A-6. Measured pavement surface profile with base failure.

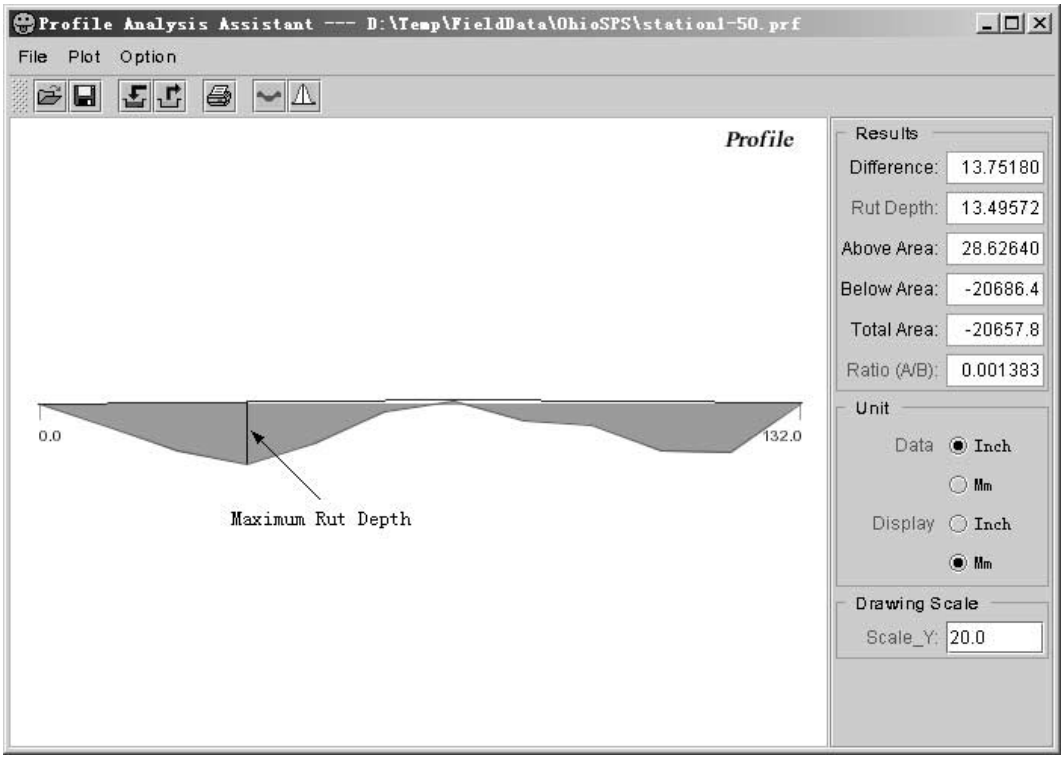

Figure A-7. Surface profile and distortion parameters for base failure.

$$A = A_P + A_N = 28 + (-20,686) = -20,658\text{mm}^2 \quad \text{(A-19)}$$

$$R = |A_P/A_N| = |28/(-20,686)| = 0.0014 \quad \text{(A-20)}$$

Equations A-3, A-4, and A-5 are used to calculate the three critical coefficients C_1, C_2, and C_3, respectively.

$$\begin{aligned} C_1 &= (-858.21)D + 667.58 \\ &= (-858.21) \times 13.5 + 667.58 \\ &= -10,918.3\text{mm}^2 \end{aligned} \quad \text{(A-21)}$$

$$\begin{aligned} C_2 &= (-1,509.0)D + 287.78 \\ &= (-1,509.0) \times 13.5 + 287.78 \\ &= -20,659.3\text{mm}^2 \end{aligned} \quad \text{(A-22)}$$

$$\begin{aligned} C_3 &= (-2,120.1)D - 407.95 \\ &= (-2,120.1) \times 13.5 + 407.95 \\ &= -29,029.3\text{mm}^2 \end{aligned} \quad \text{(A-23)}$$

Conditions in Equations A-6 and A-7 are checked. The first condition is not satisfied.

$$R = 0.0014 \text{ (which is not greater than 0.05)} \quad \text{(A-24)}$$

There is no need to check the second condition. Failure did not occur in the HMA layer.

Also, note that no curvature reversal is seen in the profile plot.

The condition in Equation A-8 is checked and is satisfied.

$$\begin{aligned} A = -20,658 &\text{ (which is greater than} \\ &[C_2 + C_3]/2, \text{ or } [-20,659 - 29,029]/2, \\ &\text{or } -24,844\text{mm}^2\text{)} \end{aligned} \quad \text{(A-25)}$$

Therefore, the failure occurred in the base layer.

It should be noted that the measured data used in this example were chosen only to demonstrate the use of the criteria. The measurement interval of 300 mm (12 in.) is not recommended in practice. Use of such a large interval may cause the loss of features for HMA failure.

8 REPORT

Report the exact pavement location, date, time, weather, and operator(s).

Report the layer in which pavement deformation has occurred, along with potential remedial action options based on the failure layer.

The **Transportation Research Board** is a unit of the National Research Council, which serves the National Academy of Sciences and the National Academy of Engineering. The Board's mission is to promote innovation and progress in transportation by stimulating and conducting research, facilitating the dissemination of information, and encouraging the implementation of research results. The Board's varied activities annually draw on approximately 4,000 engineers, scientists, and other transportation researchers and practitioners from the public and private sectors and academia, all of whom contribute their expertise in the public interest. The program is supported by state transportation departments, federal agencies including the component administrations of the U.S. Department of Transportation, and other organizations and individuals interested in the development of transportation.

The National Academy of Sciences is a private, nonprofit, self-perpetuating society of distinguished scholars engaged in scientific and engineering research, dedicated to the furtherance of science and technology and to their use for the general welfare. Upon the authority of the charter granted to it by the Congress in 1863, the Academy has a mandate that requires it to advise the federal government on scientific and technical matters. Dr. Bruce M. Alberts is president of the National Academy of Sciences.

The National Academy of Engineering was established in 1964, under the charter of the National Academy of Sciences, as a parallel organization of outstanding engineers. It is autonomous in its administration and in the selection of its members, sharing with the National Academy of Sciences the responsibility for advising the federal government. The National Academy of Engineering also sponsors engineering programs aimed at meeting national needs, encourages education and research, and recognizes the superior achievements of engineers. Dr. William A. Wulf is president of the National Academy of Engineering.

The Institute of Medicine was established in 1970 by the National Academy of Sciences to secure the services of eminent members of appropriate professions in the examination of policy matters pertaining to the health of the public. The Institute acts under the responsibility given to the National Academy of Sciences by its congressional charter to be an adviser to the federal government and, upon its own initiative, to identify issues of medical care, research, and education. Dr. Kenneth I. Shine is president of the Institute of Medicine.

The National Research Council was organized by the National Academy of Sciences in 1916 to associate the broad community of science and technology with the Academy's purpose of furthering knowledge and advising the federal government. Functioning in accordance with general policies determined by the Academy, the Council has become the principal operating agency of both the National Academy of Sciences and the National Academy of Engineering in providing services to the government, the public, and the scientific and engineering communities. The Council is administered jointly by both the Academies and the Institute of Medicine. Dr. Bruce M. Alberts and Dr. William A. Wulf are chairman and vice chairman, respectively, of the National Research Council.

Abbreviations used without definitions in TRB publications:

AASHO	American Association of State Highway Officials
AASHTO	American Association of State Highway and Transportation Officials
ASCE	American Society of Civil Engineers
ASME	American Society of Mechanical Engineers
ASTM	American Society for Testing and Materials
FAA	Federal Aviation Administration
FHWA	Federal Highway Administration
FRA	Federal Railroad Administration
FTA	Federal Transit Administration
IEEE	Institute of Electrical and Electronics Engineers
ITE	Institute of Transportation Engineers
NCHRP	National Cooperative Highway Research Program
NCTRP	National Cooperative Transit Research and Development Program
NHTSA	National Highway Traffic Safety Administration
SAE	Society of Automotive Engineers
TCRP	Transit Cooperative Research Program
TRB	Transportation Research Board
U.S.DOT	United States Department of Transportation

THE NATIONAL ACADEMIES

Advisers to the Nation on Science, Engineering, and Medicine

National Academy of Sciences
National Academy of Engineering
Institute of Medicine
National Research Council